Sr–Pb isotopes signature of Lascar volcano (Chile): Insight into contamination of arc magmas ascending through a thick continental crust

N. Sainlot, I. Vlastélic, F. Nauret, S. Moune, F. Aguilera

Sr-Pb isotopes signature of Lascar volcano (Chile): Insight into contamination of arc magmas ascending through a thick continental crust

[1]N. Sainlot, [1]I. Vlastélic, [1]F. Nauret, [1,2] S. Moune, [3,4,5] F. Aguilera

[1] Université Clermont Auvergne, CNRS, IRD, OPGC, Laboratoire Magmas et Volcans, F-63000 Clermont-Ferrand, France

[2] Observatoire volcanologique et sismologique de la Guadeloupe, Institut de Physique du Globe, Sorbonne Paris-Cité, CNRS UMR 7154, Université Paris Diderot, Paris, France

[3] Núcleo de Investigación en Riesgo Volcánico - Ckelar Volcanes, Universidad Católica del Norte, Avenida Angamos 0610, Antofagasta, Chile

[4] Departamento de Ciencias Geológicas, Universidad Católica del Norte, Avenida Angamos 0610, Antofagasta, Chile

[5] Centro de Investigación para la Gestión Integrada del Riesgo de Desastres (CIGIDEN), Av. Vicuña Mackenna 4860, Macul, Santiago, Chile

* Corresponding author: natacha.sainlot@uca.fr

Abstract

In the Central Volcanic Zone of the Andean cordillera (CVZ), thickening of the continental crust 30 Ma ago led to the production of increasingly differentiated magmas. Better constrain on the interactions between ascending magmas and the thick continental crust are needed to understand the contamination processes and their implications on the geochemical diversity of arc magmas.

Lascar volcano figures among the most active Quaternary volcano of the CVZ and yet geochemical studies on its volcanic products remain scarce. We lead major-, trace elements and Pb-Sr isotopes measurements on 10 Lascar samples representative of the different petrologic types (andesitic to dacitic) in order to better characterize the Pb-Sr isotopic signature and diversity of Lascar magmas yet defined based on only 8 samples.

$^{206}Pb/^{204}Pb$ (18.770-18.823), $^{207}Pb/^{204}Pb$ (15.636-15.655), $^{208}Pb/^{204}Pb$ (38.711-38.809) and $^{87}Sr/^{86}Sr$ isotope ratios (0.705731-0.706564) show small variations within the previously defined isotopic field of Lascar. In Pb-Sr or Pb-Pb isotope space, the data points show a triangular distribution that requires the contribution of at least three end-member components at the source of Lascar magmas. We built up a two-stage three-components assimilation and fractional crystallization model (AFC) that reproduces the entire diversity of Lascar magmas. It allows us to geochemically constrain the three end-member components compositions : (**BA**) a common mantellic source with low $^{87}Sr/^{86}Sr$ (<0.70575), low $^{206}Pb/^{204}Pb$ (<18.768), $^{207}Pb/^{204}Pb$ (<15.637) and $^{208}Pb/^{204}Pb$ (<38.711) (**EB**) a lower crust and/or slab component radiogenic in Sr ($^{87}Sr/^{86}Sr$ >0.70656) and in Pb ($^{206}Pb/^{204}Pb$ >18.82 ; $^{207}Pb/^{204}Pb$ > 15.647 ; $^{208}Pb/^{204}Pb$ > 38.79), (C) a felsic upper continental crust (> 65.1 wt% of SiO_2) with similar Sr-Pb isotope composition as **EB** ($^{87}Sr/^{86}Sr$ > 0.70643; $^{206}Pb/^{204}Pb$ >18.823 ; $^{207}Pb/^{204}Pb$ >15.655 ; $^{208}Pb/^{204}Pb$ > 38.809). Both **BA** and **EB** components occur in lavas with <57 wt.% SiO_2.

This model predicts that Lascar magmas assimilated ≤ 30 % of lower crust and ≤ 29 % of upper crust. Our conclusions are in good agreement with the CVZ literature that reports the contribution of three ubiquitous end-member components at the source of CVZ magmas, with similar natures and origins.

Introduction

Earth mantle and crust constantly interact and exchange materials through different processes. Cyclic production and recycling of the oceanic lithosphere is one of those main processes, and is accountable for the formation of volcanic arcs in subduction settings. Andean subduction has been particularly studied for the diversity of its magmatism, geodynamics and geochemistry (James et al., 1981; Wörner et al., 2005; Mamani et al., 2008; Ancellin et al., 2017). The geochemical variability of magmas in subduction context has been ascribed to the heterogeneity of the mantellic source (Francallanci et al., 1989; Wendt et al., 1999 ; Hochstaedter et al., 2000; Hofmann et al., 2003), the variable input of melts and fluids derived from the slab and melt extraction from distinct mantle lithologies (Spiegelman&Kelemen, 2003 ; Rawson et al., 2016). Crustal contamination and fractional crystallization processes (AFC) are further liable for magma differentiation and diversity. In the Andean cordillera that spreads on 7000 km, the Central Volcanic Zone (CVZ) segment is well suited for studying continental subduction-related magmatism and magma-crust interactions. Indeed, CVZ magmas are characterized by overall enriched geochemical signatures (radiogenic in Sr, Pb, Nd, and LREE/HREE fractionation) (Mamani et al., 2010) in comparison to the depleted MORB mantle. Subducted sediments, sub-continental tectonic erosion (Stern et al., 1991; Kay et al., 2005) or the enriched subcontinental lithosphere (Rogers&Hawkesworth, 1989; Davidson et al., 1991), all may participate to the enriched signature of Andean magmas but are not considered as the main factors controlling CVZ magma geochemical signature (Kay et al., 1991; Mamani et al., 2010). In fact, the particular geochemical signature of Central Andean magmas is shown to be mostly the result of the interaction of mantle-derived magmas with a composite crust that grows importantly since 30 Ma (Harmon&Barreiro, 1984; Hildreth&Moorbath, 1988; Davidson et al., 1991; Kay et al., 1991; Mamani et al., 2010; Kay et al., 2014). The Central Andean composite crust is nowadays the thickest of the Andean cordillera, reaching more than 75km (Mamani et al., 2010). It is admitted that intermediate to silica-rich magmas emitted in the CVZ are the result of physica-chemical processes such as crustal assimilation coupled with fractional crystallization (AFC) and melting processes (Davidson et al., 1990). These processes are known to operate from the melting zone where primitive mafic magmas are produced, up to different levels of the continental crust where magmas are stored and then extracted (Bachmann&Bergantz, 2008; Freymuth et al., 2015). Differentiated magma emissions occur more often in arc context in comparison to other geodynamical context (hotspots, ocean ridge) and are taken responsible for arc stratovolcanoes unpredictable activity alternating long dormancy periods and violent explosive eruption (Denlinger&Hoblitt, 1999).

Lascar volcano (Chile) has been the concern of previous geochemical studies (Harmon&Barreiro, 1984; Hilton et al., 1993; Déruelle et al., 1996; Matthews et al., 1999; Risarcher&Alonso, 2001; Rosner et al., 2003; Mamani et al., 2008; Tassi et al., 2009; Menard et al., 2014). Particularly, it has been shown that Lascar magmas interact with buried gypsum from paleosalars underlying the Andean Cordillera and outcropping in the Cordillera del Sal, West of Lascar volcano (Risarcher&Alonso, 2001). These interactions between magmas and continental crust components lead us to investigate Lascar magma geochemistry and its possible interaction with the thick continental crust.

Our study aims at understanding the andesitic and dacitic magmas relationship in a volcanic arc context, during the whole period of activity of Lascar volcano from 26.5 ky to the last major eruption in 1993, and the processes that could account for the large heterogeneity of andesites. Major and trace elements contents as well as Sr-Pb isotopic compositions of Lascar magmas lead us to conclude that at least two different mafic, presumably deep sources, are responsible for the large range of andesitic compositions. Moreover, the contamination of these mafic andesitic magmas by the upper local basement, via AFC, appears to be the main process that governs dacitic magma formation in the shallow levels of the crust. These dacitic magma bodies are mobilized during the large eruption events (vulcanian to plinian). Extensive continental crust/magma interaction inevitably tends to wipe off mantellic signature in emitted magmas.

Geological context

Lascar is a stratovolcano located in northern Chile (23°22’ S/67°44’W/5590m), Est of Salar de Atacama in the Antofagasta area, on the western margin of the Andean altiplano (Fig.1) and results from the Nazca plate subduction (<60 Ma) under the South-American one (7-9 cm/y, 25° (Dorbath&Paul, 1996). Considered as the most active volcano of northern Chilean Andes, Lascar figures among the 44 potentially active edifices of the CVZ that extends from Northern Chile to North-West of Argentina, South-West of Bolivia and Southern Peru (De Silva and Francis, 1991; Stern et al., 2004) and among the 56 volcanoes of Chile with proved (dated or observed) historical eruptions (Global Volcanism Program).

Lascar volcano composite stratocone is elongated on a WSW-ENE axis (Matthews et al., 1999) and include two distinct edifices: the active east one and the dormant west one. Indeed, during stage I of Lascar stratocone formation (<43 ka), the active zone was constrained in the eastern cone and Lascar had a mafic andesitic activity. It shifted during stage II to the west with a global silicic andesitic to dacitic activity of lava dome building and ignimbrite formation (Soncor ignimbrite at 26,45 ka). Stage III of activity consisted in developing the western stratocone over

Soncor event, and culminated with Tumbres event (9,2 ka) characterized by andesitic scoria flows and crater collapses. Finally, the active zone shifted to the east during stage IV of andesitic activity, which consisted in building the three summit nested craters aligned on a E-W axis and observable nowadays (Richter et al., 2018) (crater A, B and C from W to E (Zeeuw-van Dalfsen et al., 2017)). Crater A is the seat of the current activity. Significant morphological and structural changes of the active crater occurred during the historical period (Matthews et al., 1997)) such as apparition of arcuate fractures along the crater rims, E-W faults crossing along the active crater since 1993 eruption (Pavez et al.,2006), small-scale subsidence and asymmetric horizontal displacements of all summit craters (Richter et al., 2018). However, the current locus of activity remains quite stable through time.

Lascar has been active for the past 220 ky and emitted about 30-40 km^3 of magma (Gardeweg et al., 1998). It lies on Devonian to early Carboniferous sandstones (Lila formation), Permian volcanic rocks and granites (Cas formation) and Permo-Trias volcanic products (Peine Strata et Cerro Negro Strata) (Gardeweg et al., 1998). Occurrence of coated gypsum on volcanic ash samples at Lascar revealed the presence of Tertiary gypsum deposits of the Cordillera de la Sal formations at depth (Risarcher & Alonso, 2001).

Geochemical studies on Lascar volcano are scarce in spite of its regular volcanic activity with 27 eruptions reported between 1848 and 2007, the nearly continuous passive degassing of the active crater and its active hydrothermal system. It emits calk-alkali products with composition ranging from basaltic-andesitic to dacitic. Eruption products are mainly two-pyroxene andesites and dacites with few hornblende dacites found in the Soncor flow products. Plagioclase phenocrysts are dominant in the mineral assemblage of Lascar eruptive products followed by orthopyroxene, augite, magnetite, ilmenite as well as minor hornblende, quartz and olivine (Matthews et al., 1994). Among the 162 samples previously studied (Pichler et al., 1968; Siegers et al., 1969; Deruelle et al., 1982; Hilton et al., 1993; Matthews et al., 1994; Matthews et al., 1999; Rosner et al., 2003; Mamani et al., 2010; Menard et al., 2014; Grockes et al., 2016), 107 are identified as andesites, 40 as dacites and 2 as rhyodacites gathering lavas, pumices and scorias. Petro-geochemical evidences suggest that Lascar magmas are generated by combined processes of plagioclase- and pyroxene-dominated fractional crystallization, periodic magma mixing and crustal contamination (Matthews et al., 1994). Lascar magmatic system at depth is composed of a 6km-depth open-system reservoir regularly fed with mafic magma injections leading to a complex zoned magma chamber (Matthews et al., 1999).

Since 1984, Lascar displays a cyclic activity (Mather et al., 2004) with repetition of dome formation, subsidence, crater collapse, magmatic system suppression and vulcanian to plinian

explosion (September 1986, Febuary 1990, April 1993) (Matthews et al., 1997) with eruptive column reaching 25 km high. The last major eruption of Lascar volcano (VEI 4), the 19^{th} – 20^{th} of April in 1993, emitted more than 0,1 km^3 of volcanic products (Gardeweg et al., 1998, Tassi et al., 2009). Few months before this plinian eruption, degassing pathway obstructed and overpressure was released through minor explosions in the active crater. The last eruption occurred the 4^{th} of April, in 2013 (Sernageomin). Small-scale phreatic explosions occurred at Lascar in 2015 (Gaete et al., 2019).

Samples and analytical methods

Samples include 10 volcanic rocks that encompass a large diversity of Lascar products in terms of rock type (lava, scoria, and pumice), composition (andesitic to dacitic), and age (Soncor eruption 26.45ky; Tumbre eruption 9.2ky; 1993 eruption) (Supplementary material, Fig. 2). Analysis were all carried at Laboratoire Magmas et Volcans, Clermont-Ferrand, with 7 new samples (6 andesites and 1 dacite) characterized for major-, trace- and Pb-Sr isotopic compositions and 3 andesitic samples from (Menard, PhD, 2014; unpublished) analyzed for Pb isotopes. In the literature, 162 samples are analyzed in terms of major- and trace element compositions whereas the Pb and Sr isotopic composition has only been measured on 8 and 17 samples only, respectively. Gathering Lascar data (this study + literature data), Lascar database is composed of 113 andesites and 41 dacites. The 10 new Pb-Sr isotopic data double the existing Pb-Sr isotope database on Lascar eruptive products.

Samples were sawn, crushed using a BB 250 XL Retsch jaw crusher and reduced into a micrometric (<80 µm) homogeneous powder in an agate bowl using a planetary mill (PM 100 Retsch). Both jaw crusher and agate bowl were pre-contaminated with each Lascar sample prior to the crushing and pulverizing steps. Major elements concentrations were measured with ICP-AES after dissolution of 100 mg of each sample by alkaline fusion. In order to quantify the amount of interstitial water H_2O^+, rock powders are weighted before and after exposition at 110°C during 2 hours. H_2O^- is estimated following the same methodology after another 1 hour of exposition at 1000°C, which allows quantifying the total amount of structural water. Major oxide normalization takes into account this volatile content. Trace element concentrations and Sr-Pb isotopic composition are measured on the same dissolution: 100 mg of each sample was dissolved in concentrated HNO_3 and HF acids (ratio 1:3). After evaporation, the fluoride residue was reduced by repeated additions and evaporations of a few drops of 7M HNO_3. Stock solutions were prepared adding 3x10 ml of 7M HNO_3. Daughter solutions were prepared by taking 2.4g from the stock solution. These new solutions were evaporated at 75°C, and the dry

residue was dissolved in 30 ml 0,5M HNO_3 and homogenized during 12h at 60°C. Trace elements concentrations are obtained by ICP-MS (Agilent 7500) measurements on daughter solutions. Repeated analysis of synthetic multi-element standard CMS (Inorganic Venture) and rocks standards BE-N, JA-1 and BCR-2 are used to evaluate the accuracy and the reproducibility of major and trace elements measurements. Internal reproducibility (2σ) is 5% for most elements. External reproducibility (repeated analysis of standards) is better than 10% for most elements, except for some chalcophile and siderophile elements. The difference between JA-1 and BCR-2 standards measured values and references values (GeoRem, 2019) is within the external error.

Pb and Sr were isolated from stock solutions following the protocol described by (Pin et al., 2014), and their isotopic compositions were performed on MC-ICP-MS (Neptune +) and Thermal Ionization Mass Spectrometry (TIMS, Triton, ThermoScientific), respectively. Pb isotopic compositions are corrected for mass fractionation by adding a solution of the NIST SRM 997 Tl standard to the samples before analyses. Measurements are normalized to the recommended values of the international NBS 981 standard (Todt et al., 1996). Total procedural blanks contain less than 0.1 ng of Pb (<0.05% of the total amount of Pb loaded on the column). Sr isotopic compositions were carried in static mode on single Re filaments. Sr isotopic data were normalized to the recommended value of the NIST 987 standard ($^{87}Sr/^{86}Sr = 0.710245$).

Results

Major elements

Major elements concentrations of Lascar bulk rocks are reported in Supplementary Materials. Lascar eruptive products define a calk-alkaline series with SiO_2 content between 57.6 wt% and 65.1 wt% (Fig.3) with 9 andesites and 1 dacites. Most major elements (2.0 wt% <MgO<5.0 wt%; 3.3 wt% <CaO< 7.4 wt%; 14.2 wt% <Al_2O_3< 17.1 wt%) are negatively correlated to the silica content except Na_2O and K_2O (Fig.2). These trends reveal the fractionation of olivines, clinopyroxenes, Fe-Ti oxides and plagioclases (Matthews et al., 1999). Major elements contents measured in our samples span nearly the entire compositionnal field of Lascar volcano reported in literature (55.3-67.7 wt% SiO_2, 1.58-5.81 wt% MgO, 3.10-7.67 wt% CaO and 14.3-18.2 wt% Al_2O_3).

Trace elements

Trace elements concentrations are reported in Supplementary Materials. Trace elements concentrations diagram of Lascar bulk rocks normalized to primitive mantle (Fig.4) is consistent with literature data from the CVZ. It shows typical arc-related patterns mostly

defined by high content in large ion lithophile elements (Cs, Rb, Ba) and U, Th, Pb with concentrations that reach more than 100 times those of the primitive mantle (Sun&McDonough, 1995). High field strength elements display negative anomalies (Nb (7-11 ppm); Ti (3765-5240 ppm)). These elements remain enriched with content 5 to 10 times primitive mantle values. Heavy rare earth elements (HREE)- and middle rare earth elements (MREE) content are depleted relative to light rare earth elements (LREE) content. We observe an increase of the $(La/Sm)_N$ ratio (from 2.8 to 3.7) with the increase of the silica content (Fig.5). Inversely, $(Dy/Yb)_N$ ratio (MREE/HREE) slightly decreases with silica content (1.30 to 1.13), which has been related to the fractionation of amphibole during magma differentiation (Davidson et al., 2007). In La/Yb vs. Sm/Yb diagram (Fig. 6a), a vertical trend reveals amphibole fractionation as MREE and HREE do not fractionate from each other during amphibole fractionation ($D^{MREE}_{Amph} \sim D^{HREE}_{Amph}$). Differently, La content increases ($D^{LREE}_{Amph} < D^{HREE}_{Amph}$) as amphibole crystallizes (Tiepolo et al., 2007).

Compatible elements contents (V, Cr, Sr) decrease with the silica content (178 to 78 ppm, 106 to 30 ppm and 728 to 334 ppm, respectively) following plagioclase, pyroxene and amphibole crystallization (Matthews et al., 1994) and is in good agreement with literature data (12<V<335; 0.2<Cr<264; 139<Sr<1939) (Fig.5). Sr content of Lascar bulk rocks reveal (1) a flat trend with increasing silica content and (2) a second trend toward Sr-rich content while increasing the differentiation index (samples from Mamani et al., 2010; Fig. 5). The Sr-rich trend gathers only andesitic magmas (SiO_2 < 63 wt%). Incompatible elements (Th, Ba) contents increase with differentiation (5 to 14 ppm and 344 to 543 ppm, respectively while remaining within the range of literature values (4<Th<24 ppm and 218<Ba<1871 ppm). We observe a geochemical heterogeneity of the andesitic terms (between 56 and 63 wt% SiO_2) (Fig.5). Incompatible trace element ratios Th/La, Ba/U and Rb/Th vary from 0.25 to 0.58, from 115 to 259 and from 8.08 to 9.60 respectively, in good agreement with literature values (0.21<Th/La<1.00 ; 66<Ba/U<631 and 1.45<Rb/Th<15.84). Th/La ratio positively correlates with silica content while Ba/U and Rb/Th ratios display a negative correlation with silica content. Both Th/La and Ba/U ratios evolutions with differentiation partly reveal the fractionation of amphibole (Nauret et al., 2017). Because amphibole is rarely a phenocryst phase of Lascar magmas, amphibole may fractionate at depth (Davidson et al., 2007).

Pb-Sr isotopes

Pb-Sr isotopic compositions of Lascar eruptive products are reported Table 4. $^{206}Pb/^{204}Pb$ ratios range between 18.77 and 18.82, $^{207}Pb/^{204}Pb$ ratios between 15.64 and 15.65 and $^{208}Pb/^{204}Pb$ ratios between 38.71 and 38.80. $^{87}Sr/^{86}Sr$ isotope ratio range between 0.705731 and 0.706564.

Our data are consistent with the literature data on Lascar volcano with $18.740<^{206}Pb/^{204}Pb<18.840$; $15.620<^{207}Pb/^{204}Pb<15.659$; $38.660<^{208}Pb/^{204}Pb<38.842$ and $0.70560<^{87}Sr/^{86}Sr<0.70719$ (Harmon et al., 1984; Hilton et al., 1993 ; Déruelle et al., 1996; Rosner et al., 2003; Mamani et al., 2010). The $^{207}Pb/^{204}Pb$ ratios of andesites cover the entire range of variation of Lascar magmas, from 15.62 to 15.66. Increasing the differentiation index, dacites display more homogeneous $^{207}Pb/^{204}Pb$ between 15.650 and 15.655.

$^{206}Pb/^{204}Pb$ ratios of Lascar eruptive products are positively correlated to $^{207}Pb/^{204}Pb$ and $^{208}Pb/^{204}Pb$ (Fig.7). In this figure, we report the compositions of the subducted component (i.e. Nazca plate, Unruh&Tatsumoto, 1974), the local basement (Upper continentale crust composed of the Quepe Strata and the Cordon de Lila, Mamani et al., 2008), the average composition of the lower continental crust (Weber et al., 2002) and the DMM (Depleted MORB Mantle, Rehkamper & Hofmann 1997). Lascar bulk rocks plot in the field of the local basement composition, in the center of a triangle formed by the DMM, the radiogenic upper crust and a third pole less radiogenic in Pb.

Using different geochemical parameters ($^{206}Pb/^{204}Pb$, $^{207}Pb/^{204}Pb$, $^{208}Pb/^{204}Pb$, $^{87}Sr/^{86}Sr$, SiO_2), we observe a triangular shape, which results from the geochemical heterogeneity of the andesitic terms (Fig.8). This ternary distribution cannot be explained by a simple binary mixing process (Schiano et al., 2010) but could result from a more complex process involving at least three end-member components at the source of Lascar magmas (Keay et al., 1997).

Discussion

1. **Three ubiquitous end-members at the source of CVZ magmas**

Several isotope spaces, including $^{207}Pb/^{204}Pb$ (and $^{208}Pb/^{204}Pb$) vs. $^{206}Pb/^{204}Pb$ space and $^{87}Sr/^{86}Sr$ vs. $^{206}Pb/^{204}Pb$ (Fig.9) show a triangular dispersion of quaternary magmas emitted in the CVZ (data compilation by Mamani et al., 2010), including Lascar data. This triangular distribution is also observable at Lascar scale (Fig.7&8). Such a distribution is a robust evidence for the presence of three ubiquitous end-members at the source of all CVZ magmas (Harmon&Barreiro, 1984; Godoy et al., 2014; Freymuth et al., 2015; Blum-Oeste&Wörner, 2016). Among them, Blum-Oeste&Wörner (2016) identified two mafic end-members formed by deep processes; a typical basaltic andesite here referred as **BA** component, and an enriched basalt here referred as **EB** component. This overall andesite geochemical heterogeneity in arc magmas may be explained by the chemical variability of the mantle source, the recurrent recycling of slab components (McCulloch and Gamble, 1991; Plank and Langmuir, 1998; Elliott, 2003; Turner and Langmuir, 2015b) and the complex interaction between melt and

peridotite in melt extraction channels (Cann et al., 1997; Rawson et al., 2016). However, at the CVZ scale, the geochemical diversity of low-silica magmas is often explained by ; **(1)** lower crust contamination (Harmon&Barreiro, 1984; Hildreth&Moorbath, 1988; Davidson et al., 1990; Vatin-Pérignon et al., 1991; Godoy et al., 2014). Magmas interaction with the lower continental crust at depth is recorded by trace elements (Davidson et al., 1990; Davidson et al., 1998; Godoy et al., 2014), He (Hilton et al., 1982), O, Pb and Sr isotopes (Harmon&Barreiro, 1984; Godoy et al., 2014; Freymuth et al., 2015). Geochemical data on CVZ magmas converge toward a common interpretation; typical mantellic arc magmas ascent from their melting zone to the lower crustal zone where they are stored, differentiate and assimilate country rocks in deep "MASH zones" (Melting, Assimilation, Storage, Homogeneization (Hildreth&Moorbath, 1988; Wörner et al., 1988; Wörner et al., 1994; Mamani et al., 2008; Godoy et al., 2014, Freymuth et al., 2015). **(2)** The chemical variability of the mantle source swollen by the recurrent recycling of slab components and sediments (McCulloch and Gamble, 1991; Vatin-Pérignon et al., 1991; Plank and Langmuir, 1998; Kay et al., 2002; Elliott et al., 2003; Goss et al. 2013; Turner and Langmuir, 2015b). However, Mamani (2010) argued that the hyperaridity of the western Andean slope since the late Oligocene/Miocene (Rech et al., 2006; Hartley et al., 2007), the presence of the Coastal Cordillera that prevents sedimentary transport into the ocean (Allmendinger et al., 2005) and the absence of accretion prism (von Huene et al., 1999), all argue against the presence of significant amounts of sediments in the subduction zone to enrich Andean magmas. Thus, lower- to mid crustal contamination of mantellic magmas through deep mash zones storage likely explains the geochemical heterogeneity of low-silica lavas.

At Lascar, the basic composition of the Andean lower crust (Godoy et al., 2014) supports the hypothesis that temporary storage/assimilation of mantle derived magmas within the lower crust might shift the geochemical trend toward low-silica and radiogenic (Pb-Sr) compositions. In fact, this hypothesis is supported by petrologic and petrographic analysis of Lascar Piedras Grande andesite which is interpreted to form by remobilization and melting of an igneous protolith following the new injection of hydrous mafic magma (Matthews et al., 1999). This latter is thought to have evolved in the lower crust by high-pressure fractionation and lower crust assimilation (Matthews et al., 1999).

Finally, the evolution towards silica-rich compositions (**RD**, Blum-Oeste&Wörner, 2016) is ascribed to shallow differentiation by assimilation of the upper continental crust (AFC) (Mamani et al., 2008; Blum-Oeste&Wörner, 2016; Nauret et al., 2017). Indeed, magmas assimilation of the upper crust by AFC processes is prone to increase the silica content of magma by differentiation as well as their Sr-Pb isotopic composition. The chemical and isotopic

diversity of high-silica arc magmas at the CVZ scale is explained by the local heterogeneity of the Andean upper continental crust (Wörner et al., 1992; Mamani et al., 2008, 2010).

2. At least 2 mafic end-members at the source of Lascar magmas

Three ubiquitous end-members have been identified at the source of all CVZ magmas. At a smaller scale, the study of Lascar lavas allow us to constrain how the 3 end-members interplay within the plumbing system of one of the most active stratovolcanoes of the CVZ.

At Lascar, we observe a strong geochemical heterogeneity of the less differentiated terms (basaltic andesites and andesites). The mineral assemblage (Matthews et al., 1999) of Lascar andesites (Plagioclase + Clinopyroxene + Orthopyroxene + Amphibole + Oxide + Biotite with minor apatite and olivine) is not able to efficiently fractionate incompatible elements (i.e, Rb, Th) as their partition coefficient is <<1. Thus, the large range of variation of incompatible elements ratios (Fig.5) in the less differentiated magmas (<63 wt% SiO_2) cannot result from fractional crystallization in a closed system (Davidson et al., 1988). This heterogeneity of andesite terms is ascribed to the heterogeneity of mafic end-members at the source of andesite magmas.

Moreover, the two flat- (1) and increasing- (2) trends in Sr vs. SiO_2 diagram (and Ba vs. SiO_2) (Fig. 5) could not respond to a simple fractional crystallization process as Sr content commonly decreases with fractional crystallization. The absence of Eu positive anomaly (Eu/Eu* ratio >1) precludes plagioclase accumulation as being the cause of these high Sr values and the overall Sr variability at SiO_2 < 63 wt%. This is consistent with the study of Matthews et al. (1994) that estimated a low extent of crystallization (≤11.5%) of predominantly plagioclases and pyroxenes in Lascar magmas. Other processes have to be considered to explain these trace elements variabilities in low-silica magmas. Samples which exhibit strong Sr (up to 1716 ppm) and Ba (up to 1676 ppm) enrichments also display low Ni and Cr contents (<65 and <168 ppm, respectively), high Sr/Y ratio (from 84 to 697) and LILE/HFSE ratios with $(Ba/Nb)_N$ up to 18,4. These geochemical characteristics are typical of the common **EB** end-member at the source of CVZ magmas (Bloom-Oeste&Wörner, 2016). Thus, Lascar magmas may have interact with the **EB** pole, providing an explanation to Lascar andesite heterogeneity. This idea is supported by the Pb-Sr isotopic heterogeneity of Lascar andesites (Fig.7), which is a strong clue for the existence of this deep source heterogeneity underneath Lascar volcano.

Another hypothesis is based on the petrographic analysis of Lascar products, which allows the identification of three processes occurring in the plumbing system of Lascar volcano; (a) fractional crystallization (b) assimilation of the country rock and (c) magma mixing between a felsic and a mafic end-member (Matthews et al., 1994, 1999). The latest is notably suggested

following the observation of zoned plagioclases and pyroxenes, disequilibrium textures and the occurrence of mafic inclusions. Mixing process could be liable for the low-silica magmas heterogeneity as new mafic injections in a dacitic reservoir are prone to trigger eruption by rapid magma mixing (Spark et al., 1977; Murphy et al., 1998; Snyder et al., 1999) with little fractional crystallization of plagioclase and/or limited assimilation of the country-rock. The flat Sr trend (1) could finally reflects a small extent of plagioclase fractionation balanced by an input of Sr from a Sr-rich country-rock formation (AFC).

3. Evidence for crustal contamination of Lascar dacite

Several observations reported in literature provide clues in favor of crustal assimilation/mixing processes being responsible for the geochemical diversity of Lascar magmas. First, Risarcher&Alonso (2001) found large amounts (an estimation of 700,000 tons) of soluble $CaSO_4$ coated on ash grains emitted during the three days of the 1993 plinian eruption. This has been attributed to the massive recycling of buried Cenozoic evaporates underneath Lascar volcano, accounting for the interaction between magmas and the upper crustal basement of Lascar volcano. In a similar way, calcsilicates xenoliths occur in at least five eruptive products emitted by Lascar volcano, namely the andesitic-dacitic Piedras Grandes block and ash flow, the andesitic-dacitic Soncor flow, the dacitic Capricorn lava flow, the andesitic Tumbres scoria flow and the deposits of the andesitic 1993 short-lived plinian eruption (Matthews et al., 1996). Xenoliths compositions strongly suggest that the protholith corresponds to the Upper Cretaceous Yacoraite formation that crops out in NW Argentina. This formation is composed of diverse carbonate-calcareous-dolomitic lithology but also contains shales and sandstones. Moreover, petrological studies on Lascar eruptive products (Matthews et al., 1999) suggest that the hydrous mafic magmas underwent deep-fractionation processes at high pressure (lower crust level) and evolved by lower crust assimilation processes.

Furthermore, the dataset on Lascar volcano supports the idea that crustal contamination plays a key role in dacites formation. Indeed, the decrease of highly incompatible trace elements ratios (Fig. 5), such as Rb/Th (from 14.47 to 5.21) with the increase of the silica content could not respond to a simple process of crystallization (Davidson et al., 1988). Indeed, as incompatible elements do not fractionates during fractional crystallization, this Rb/Th decrease requires the input of a genetically unrelated component with low Rb/Th ratio. A Th-rich crustal component would be a possible candidate responsible for this evolution. The evolution of Lascar magma towards radiogenic Pb and Sr composition is consistent with assimilation of the shallow radiogenic crust.

Finally, Lascar data defines a linear trend in the 1/V vs. Rb/V diagram (Fig.6b), which is used to distinguish which processes between partial melting, fractional crystallization and mixing, are responsible for the evolution of magmas compositions (Schiano et al., 2010). In this diagram, the linear trend reveals a binary mixing process (Langmuir et al., 1978) at the origin of Lascar magmas heterogeneity. Inversely, a curved distribution would have reflected a crystallization process. The linear trend formed by andesites and dacites bulk rocks from Lascar reveals mixing process as the main co-genetic link between low-silica and high-silica magmas. However, petrological and geochemical evidences clearly suggest that amphibole crystallization plays a major role. Both mixing and crystallization processes must be taken into account for the formation of dacitic magmas. This is in good agreement with Blum-Oeste&Wörner (2016) who showed that crustal melting and mixing with evolved magmas derived from the mantle wedge (**BA**) are the most likely processes to generate the **RD** end-member at CVZ scale. Thus, we propose that assimilation fractional crystallization (AFC) is the main process controlling Lascar magmas compositions. Though crustal mixing in MASH zones at lower crust depth (30-50 km) is likely to be responsible for the formation of the RD end-member at CVZ scale, Lascar magmas compositions do not tend exactly toward the common RD end-member (Blum-Oeste&Wörner, 2016). Indeed, the slight difference between the **RD** end-member and its local equivalent below Lascar volcano is thought to reflect small-scale heterogeneity of the CVZ basement and/or a shallow origin of the ubiquitous **RD** end-member. At Lascar scale, **RD** is now called **C** to emphasize on that difference.

4. AFC models

   i. Constrains on BA and EB end-members

In order to test the hypothesis of interaction between these three end-members (**BA**, **EB**, **C**) at the source of Lascar magmas, and estimate the amount of crust assimilated by Lascar volcanic products, we built up a 2-stages 3-components AFC model (DePaolo et al., 1981). First, the geochemical and Pb-Sr isotopic composition of the two end-members common in all CVZ magmas (**BA**, **EB**) and the local crustal component specific to Lascar (**C**) have to be defined.

At Lascar scale, we can isotopically constrain these three end-members; (**BA**) a typical mantellic arc magma with low $^{87}Sr/^{86}Sr$ (<0.70575), low $^{206}Pb/^{204}Pb$ (<18.768), $^{207}Pb/^{204}Pb$ (<15.637) and $^{208}Pb/^{204}Pb$ (<38.711) and (**EB**) a mafic component presumably derived from the lower crust, radiogenic in Sr (>0.706564) and in Pb (>18.82 ; > 15.647 ; > 38.79) with higher Th concentration than component A. These two compositions are best preserved in lavas with <57wt% SiO_2. The third pole (**C**) corresponds to the local basement (> 65.1 wt% of SiO_2), which is similarly radiogenic in Sr and Pb as component **EB** (> 0.70643; >18.823; >15.655; >

38.809) and displays the highest Th content (up to 14.2 ppm). However, the absence of isotopic measurements on primitive melt inclusions from Lascar and local lower crust does not allow us to further constrain geochemical signature of **BA** and **EB** end-members. Thus, we estimated generic **BA**, **EB** compositions at CVZ scale which are defined at the extremity of the triangular shaped distribution gathering all the CVZ quaternary eruptive products (Fig.9) : **BA**: $^{206}Pb/^{204}Pb$ = 16.61; [Pb] = 11ppm and $^{87}Sr/^{86}Sr$ = 0.7040; [Sr] = 100ppm; **EB**: $^{206}Pb/^{204}Pb$ = 17.70; [Pb] = 30ppm and $^{87}Sr/^{86}Sr$ = 0.7080; [Sr] = 200ppm.

ii. 2-stages 3-components AFC model

We then tested a two-stages three-components AFC model in the $^{206}Pb/^{204}Pb$ - $^{207}Pb/^{204}Pb$ - $^{208}Pb/^{204}Pb$ isotope space (Fig.10). The solutions of the model were calculated using the analytic equations from De Paolo (1981). The model includes a first binary **BA-EB** contamination step followed by a 2nd assimilation step between the hybrid **BA-EB** component and **C**. The two stages (**BA-EB** and **BAEB-C**) are thought to occur successively given the nature of the selected end-members. Indeed, magma ascension through the crust implies a first reaction of the magma with the lower crust (**EB**, MASH zones) and subsequently, the interaction of this hybrid magma with the upper part of the crust (**C**) before erupting at earth surface. AFC models are verified in all the dimensions of the considered spaces ($^{206}Pb/^{204}Pb$, $^{207}Pb/^{204}Pb$, $^{208}Pb/^{204}Pb$, $^{87}Sr/^{86}Sr$). Estimated results represent minima of the assimilation extent at Lascar as samples analyzed for Pb and Sr isotopes do not correspond to Lascar samples with extreme major and trace elements contents. This model takes into account the mineralogical assemblage (Matthews et al., 1999), the composition of the most primitive end-members (**BA** and **EB**), the composition of the crustal contaminant (**C**), the assimilation rate *r* defined by the mass ratio between assimilated and crystallized material, and the magma mass ratio *F* between the initial magma and the contaminated one. Because the upper crustal material around Lascar is highly heterogeneous, we tested several potential contaminant **C** ; a Northern Chile Paleocene intrusion (Haschke et al. 2002), a Paleozoic gneiss from the Salar de Antofalla (Lucassen et al., 2001; Siebel et al., 2001), a Northern Chile Paleozoic gneiss (Loewy et al., 2004), Cordon de Lila Proterozoic gneiss (Bock et al., 2000) and an Ordovician Antofalla intrusion (Lucassen et al., 2002). Distribution coefficients have been calculated using the partition coefficients of reference (Ewart et al., 1973; Ewart&Griffin, 1994; Bacon&Druitt, 1998) and a mineralogical assemblage of 23.2% Plagioclase + 1.2% Clinopyroxene + 0.9% Orthopyroxene + 0.6% Olivine + 0,1% Hornblende with 74.0% of matrix inferred by Matthews et al. (1999) based on the mineralogical composition of lavas from Lascar (LAS451a, LAS451b, LAS61, LAS62).

In order to reproduce the andesite geochemical variability (trend n°1), our model indicates that with F parameter ranging between 0.05 and 0.45, r should vary between 0,02 and 0.32. Lascar magmas would have assimilated between 1 and 30% of the lower crust in order to produce the observe andesite geochemical variability.

It is known that crustal contamination is not uniform and is ruled by the composition, the structure and the thermal conditions of the local crustal basement through which magmas ascent (Godoy et al., 2017). Among local upper crustal components, the Paleozoic gneiss from Salar de Antofalla displays the closest compositions to the **C** pole and would be a potential contaminant of Lascar magmas. Moreover, Cordon de Lila gneiss intrusion that has already been described as Lascar basement (Gardeweg et al., 1998) shows Pb isotopic compositions similar to the composition estimated for the contaminant and is prone to be the upper crustal component. Inversely, we notice that northern Chile Paleocene intrusion (Haschke et al. 2002) as well as the Ordovician intrusion from Antofalla domain (Lucassen et al., 2002) are not potential contaminants. Besides, studies on Lascar's neighbor San-Pedro-Linzor volcanic chain in northern Chile showed major contamination of the magmas by the Altiplano-Puna Magma Body (APMB), a large batholith settled in the upper crust (Godoy et al., 2017). They identify that Lascar volcano lies outside the APMB, which explains why Lascar magmas are mostly preserved from the APMB contamination (<10% vol.). The absence of strong connection between Lascar magmatic system and the APMB is also pointed out by the mean of magnetotelluric measurements along profiles south of Lascar, crossing the Salar de Atacama, the volcanic arc and the western border of APMB (Diaz et al., 2012). Thus, we do not consider APMB as a potential contaminant of Lascar magmas. In spite of the few data on Lascar basement and its geochemical heterogeneity, Cordon de Lila is prone to be the main contaminant of Lascar magmas. Nonetheless, Cordon de Lila Pb-Sr database is scarce and heterogeneous and cannot explain the full isotopic range of Lascar magmas, suggesting that either the entire geochemical heterogeneity of Cordon de Lila has not been sampled or another lithology is responsible for the contamination of Lascar magmas.

A generic composition of the contaminant is estimated by iteration in order to best-fit data dispersion during the 2nd step of the AFC model. The generic contaminant composition displays $^{206}Pb/^{204}Pb$, $^{207}Pb/^{204}Pb$, $^{208}Pb/^{204}Pb$ and $^{87}Sr/^{86}Sr$ values of 19.12, 15.73, 39.20 and 0.7080, respectively. These estimations are in good agreement with the geochemical signatures previously suggested for this end-member and are, based on the new and published data, the most robust constrains on the contaminant of Lascar magmas. With F parameter ranging between 0.05 and 0.45, and r varying between 0.1 and 0.3, magmas would have assimilated

between 6 and 29% of this generic upper crustal end-member. It is noteworthy that these ranges of values are obtained by running the model in all Pb-Sr isotopic spaces.

Finally, the presence of Yacoraite xenoliths in Lascar volcanic products is a strong clue for the involvement of this calcsilicate formation in the contamination of Lascar magmas. However, no Pb-Sr isotopic measurements are available for these xenoliths to better constrain the role of this potential upper crustal contaminant **C**. In such situation, we used trace elements (Nd, Ba, Rb, Sr and Pb) to model the AFC evolution of EB-BA hybrid magmas considering assimilation of Yacoraite calcsilicates (referred to as C'). LA-143 sample from Lascar (Matthews et al., 1994) is used as a starting material and the sample 92/212 from Yacoraite formation (Marquillas et al., 2011) plays the role of Lascar magmas contaminant. We tested two AFC models using 1) AFC equations from De Paolo (1981) (Fig. 11 a&b) and 2) AFC3D software (Guzman et al., 2014) (Fig. 11 c&d). To first order, results of the calculations show that Yacoraite could act as an assimilant at Lascar. The AFC trend toward Yacoraite overlaps a large range of Lascar magmas geochemical diversity (Fig. 11a&b) with ranges of variation of r and F parameters (0.1-0.3 and 0.20-0.45, respectively) consistent with previous estimations. Nonetheless, results with AFC3D software show that no common set of (r, β, ρ) is found for the considered elements, meaning that each element yields a different extent of assimilation. The inconsistency between the two models results from the fact that De Paolo (1981)'s model yields different results depending on which element is considered. It shows that the assumptions of the AFC model (e.g. constant D, same composition of primitive magma and contaminant for all samples) are too simple to account for the complexity of natural AFC processes.

Conclusions

Major-trace element concentrations and high precision Pb-Sr isotopes measurements are reported for 10 new rock samples from Lascar volcano, extending the yet limited database available for this edifice. New and published data allow us to draw several conclusions regarding magma contamination bellow Lascar and the Central Volcanic Zone (CVZ):

(1) Lascar magmas display typical arc calcalkaline series compositions from basaltic andesites to dacites. As for several arc volcanoes, Lascar magmas shows a large geochemical diversity of its low-silica (<60 wt% SiO_2) products.

(2) Combined geochemical parameters (SiO_2 content, incompatible trace element ratios, $^{87}Sr/^{86}Sr$, $^{206}Pb/^{204}Pb$, $^{207}Pb/^{204}Pb$ and $^{208}Pb/^{204}Pb$) and AFC modeling indicate that at least three end-members are involved at the source of Lascar magmas. These three

sources likely have the same origin as the three ubiquitous components identified at the regional scale of the CVZ. The geochemical signature of the upper crustal contaminant slightly varies from place to place due to the upper crust heterogeneity.

(3) Two-stages three-components AFC model reproduces the entire dispersion range of Lascar bulk rocks and allows us to better constrain end-members geochemical composition: (**BA**) a common mantellic source with low $^{87}Sr/^{86}Sr$ (<0.70575), low $^{206}Pb/^{204}Pb$ (<18.768), $^{207}Pb/^{204}Pb$ (<15.637) and $^{208}Pb/^{204}Pb$ (<38.711), (**EB**) a deep-mafic source radiogenic in Sr (>0.706564) and in Pb (>18.82 ; > 15.647 ; > 38.79), (**C**) the local upper crust (> 65.1 wt% of SiO_2) with similar Sr-Pb isotope composition as **EB** (> 0.70643; >18.823 ; >15.655 ; > 38.809).

(4) This study on Lascar and those done at the scale of the CVZ reach converging interpretations regarding the origin of the ubiquitous end-members: **BA** the mantle wedge, **EB** an enriched component (lower continental crust and/or the slab), **C** the local upper continental crust.

Figure captions

Figure 1

Location map of Lascar volcano in the Central volcanic zone in the Antofalla domain, Northern Chile, modified from (Mamani et al., 2010; Menard et al., 2014)

Figure 2

Geological map from Lascar modified from (Gardeweg et al., 1998). Localization of Lascar samples is shown.

Figure 3

K_2O, MgO, CaO and Al_2O_3 vs. SiO_2 diagram for Lascar bulk rock samples. Literature data sources : (Siegers et al., 1969; Deruelle et al., 1982; Harmon et al., 1984; Hilton et al., 1993; Matthews et al., 1994, 1999; Rosner et al., 2003; Mamani et al., 2008, 2010; Grockes et al., 2016). High K, medium K and low K fields are defined after (Peccerillo & Taylor, 1976). Same symbols as in Fig.6.

Figure 4

Primitive mantle-normalized trace element diagram (normalized values after Sun and McDonough (1989)) for Lascar bulk rock samples.

Figure 5

Trace element concentration (V, Ba, Sr, Th) and trace element ratios (Ba/U, Th/La, $(La/Sm)_N$, Rb/Th vs. SiO_2 for Lascar bulk rock samples.

Figure 6

a) La/Yb vs. Sm/Yb plot showing Lascar data. A vertical trend is accountable for amphibole fractionation (Tiepolo et al., 2007). b) 1/V vs. Rb/V diagram for Lascar bulk rocks. The linear trend highlight a binary mixing process (Schiano et al., 2010). Literature data sources : (Siegers et al., 1969; Deruelle et al., 1982; Harmon et al., 1984; Hilton et al., 1993; Matthews et al., 1994, 1999; Rosner et al., 2003; Mamani et al., 2008, 2010 ; Grockes et al., 2016).

Figure 7

(a) $^{207}Pb/^{204}Pb$ and (b) $^{208}Pb/^{204}Pb$ vs. $^{206}Pb/^{204}Pb$ diagram of Lascar bulk rocks. The isotopic fields are shown for the lower continental crust (LCC, Weber et al., 2002), the upper continental

crust (UCC, Mamani et al., 2008), the Nazca plate (Unruh & Tatsumoto, 1974), and the depleted MORB mantle (Rehkamper & Hofmann 1997). North Hemisphere Reference line (NHRL) is from (Hart et al., 1984). A, B and C are the components required to explain andesites heterogeneity. More details and references in the main text.

Figure 8

(a) $^{87}Sr/^{86}Sr$ vs. $^{206}Pb/^{204}Pb$ diagram and (b) $^{207}Pb/^{204}Pb$ vs. SiO_2 wt% diagram of Lascar bulk rocks. Suggested end-members (A, B, C) are required to explain the triangular distribution due to andesites heterogeneity. Origin of A, B, C is detailed in the text.

Figure 9

$^{87}Sr/^{86}Sr$ and $^{207}Pb/^{204}Pb$ vs. $^{206}Pb/^{204}Pb$ for Lascar bulk rocks and eruptive products from CVZ quaternary volcanoes (compilation from (Mamani et al., 2010)). CVZ volcanoes are grouped according to crustal domains. Three end-members (**BA**, **EB**, **C**) are required to explain the triangular distribution at CVZ scale. Origin of **BA**, **EB**, **C** is discussed in the main text.

Figure 10

(a) 2-stages 3-components AFC model (DePaolo et al., 1981) is presented in $^{207}Pb/^{204}Pb$, $^{208}Pb/^{204}Pb$ and $^{87}Sr/^{86}Sr$ vs. $^{206}Pb/^{204}Pb$ spaces with black lines for Lascar bulk rocks. **BA**, EB, and **C** are the three end-members required to model the whole geochemical dispersion of Lascar dataset. Trend (1) corresponds to AFC modelling between **BA** and **EB** end-members considering **EB** as the lower crust. Trend (2) corresponds to AFC modelling between diverse **BA**-**EB** mixing products and C, the upper crust. Two potential local upper crustal contaminants (Cordon de Lila and Salar de Antofalla) are considered in the second stage of the AFC modelling. Both contaminants cannot account for the $^{207}Pb/^{204}Pb$ values of Lascar bulk rocks.

Figure 11

Probing the interaction between Lascar magmas and the Yacoraite formation with different AFC models. The composition of the basaltic andesite LA-143 (Matthews et al., 1994) and the calcsilicate sample 92/212 (Marquillas et al., 2011) are used for mantle-derived magma and the Yacoraite formation, respectively. Results obtained with De Paolo (1981)'s equations are plottind in Sr/Rb vs. Rb (a) and Ba/La vs. Pb spaces (b). Both diagrams show that assimilation trends toward Yacoraite could partly account for Lascar magmas geochemistry. (c)&(d) Results obtained with AFC3D (Guzman et al., 2014) using R environment. AFC3D proposes a graphical 3D representation of ρ (mass of assimilated crust/mass of original magma) in function

of r (rate of crustal assimilation/rate of fractional crystallization) and β (recharge rate of magma replenishment/rate of assimilation) parameters that account for the concentration variations of several elements. A common set of (r, β, ρ) corresponds to potential solutions for a set of selected elements and plots in the 3D space as the intersection of the (r, β, ρ) surfaces of each element (c). These parameters are calculated for each element according to Aitcheson and Forrest (1994) based on input parameters Ca, the element concentration in the assimilant, C_m^0 the element concentration in the original magma, C_m the element concentration in the contaminated magma and, D the bulk partition coefficient of the original magma fractionating mineral assemblage. The ranges of variation (min/max) of r, F (mass of magma remaining), and β are set before running calculations as well as the zero threshold value. The zero threshold value corresponds to the allowed difference between all ρ values of the selected set of elements and should not exceed 10^{-2}.We run the model for Sr, Rb, Ba, Pb and Cr, beginning with ranges of variations of r, F and β fixed between 0 and 3 and the zero threshold at 10^{-2}. In the r-β-ρ space, the surfaces of solutions obtained for each elements are sub-parallel and do not intersect a single point, meaning that no common solution exists for the considered set of elements. If one decreases the zero threshold values and r, F, β ranges of variation, then model results converge toward a rate of assimilation of 0 (red line on Fig. 11d).

Supplementary Material

Table S1: Geochemical database (major-, trace elements and Pb-Sr isotopic compositions) gathering published and new data on Lascar volcano eruptive products (GERM database; Menard, PhD, 2014; This study).

Acknowledgements

D. Auclair, A. Gannoun, J.L. Piro contributed to data acquisition. We thank S. Guzman and an anonymous reviewer for their constructive comments, and P. Samaniego for his useful remarks and for handling the manuscript. This work benefited from the financial support from the Institut de Recherche pour le Développement (ECOS-sud project no. C11U01, P.I. O. Roche), the French Government Laboratory of Excellence initiative n°ANR-10-LABX-0006, the Région Auvergne and the European Regional Development Funds. This is Laboratory of Excellence ClerVolc contribution number 397.

References

Aitcheson S.J., Forrest A.H. 'Quantification of crustal contamination in open magmatic systems' (1994). *J. of Petrology* 35, 2, 461-488. https://doi.org/10.1093/petrology/35.2.461

Allmendinger, R.W., González G., Yu J., Hoke G., and Isacks B. (2005) 'Trench-Parallel Shortening in the Northern Chilean Forearc: Tectonic and Climatic Implications'. *GSA Bulletin* 117, 1–2, 89–104. https://doi.org/10.1130/B25505.1.

Ancellin M-A., Samaniego P., Vlastélic I., Nauret N., Gannoun A., and Hidalgo S. 'Across-Arc versus along-Arc Sr-Nd-Pb Isotope Variations in the Ecuadorian Volcanic Arc: Along-arc Ecuador' (2017). *Geochem. Geophys. Geosyst.* 18, 3, 1163–88. https://doi.org/10.1002/2016GC006679.

Annen, C. 'From Plutons to Magma Chambers: Thermal Constraints on the Accumulation of Eruptible Silicic Magma in the Upper Crust' (2009). *Earth and Planetary Science Letters* 284, 3, 409–16. https://doi.org/10.1016/j.epsl.2009.05.006.

Bachmann O., Bergantz G. 'The Magma Reservoirs That Feed Supereruptions' (2008). *Elements* 4, 1, 17-21. https://doi.org/10.2113/GSELEMENTS.4.1.17.

Bacon, C.R., Druitt T.H. 'Compositional Evolution of the Zoned Calcalkaline Magma Chamber of Mount-Mazama, Crater Lake, Oregon' (1988). *Contrib. Mineral. Petrol*. 98, 2, 224-256. https://doi.org/10.1007/BF00402114

Blum-Oeste M., Wörner, G. 'Central Andean Magmatism Can Be Constrained by Three Ubiquitous End-Members' (2016). Terra Nova 28, 6, 434–40. https://doi.org/10.1111/ter.12237.

Bock, B., Bahlburg H., Wörner G., and Zimmermann U. 'Tracing Crustal Evolution in the Southern Central Andes from Late Precambrian to Permian with Geochemical and Nd and Pb Isotope Data' (2000). *J.Geology* 108, 5, 515–35. https://doi.org/10.1086/314422.

Cann J. R., Elderfield H., Laughton A., Kelemen P. B., Hirth G., Shimizu N., Spiegelman M., and Dick H. J. 'A Review of Melt Migration Processes in the Adiabatically Upwelling Mantle beneath Oceanic Spreading Ridges' (1997). *Philosophical Transactions of the Royal Society of London. Series A: Mathematical, Physical and Engineering Sciences* 355, 1723, 283–318. https://doi.org/10.1098/rsta.1997.0010.

Davidson, Jon P., Ferguson K.M., Colucci M.T., and Dungan M.A. 'The Origin and Evolution of Magmas from the San Pedro-Pellado Volcanic Complex, S. Chile: Multicomponent Sources and Open System Evolution' (1988). *Contrib. Mineral. Petrol.*100, 4, 429–45.

https://doi.org/10.1007/BF00371373.

Davidson, Jon P., McMillan N.J., Moorbath S., Wörner G., Harmon R.S., and Lopez-Escobar L. 'The Nevados de Payachata Volcanic Region (18°S/69°W, N. Chile) II. Evidence for Widespread Crustal Involvement in Andean Magmatism' (1990). *Contrib. Mineral. Petrol*. 105, 4, 412–32. https://doi.org/10.1007/BF00286829.

Davidson, Jon P., Harmon, RS., Wörner, G. 'The source of central Andean magmas; Some considerations' (1991). *Geological Society of America Special Papers* 265, 233-244. 10.1130/SPE265-p233

Davidson J., Turner S., Handley H., Macpherson C., and Dosseto A. 'Amphibole "Sponge" in Arc Crust?' (2007). *Geology* 35, 9,787–90. https://doi.org/10.1130/G23637A.1.

Denlinger R.P., Hoblitt R.P. 'Cyclic eruptive behavior of silicic volcanoes' (1999). *Geology* 27, 5, 459-462.https://doi.org/10.1130/00917613(1999)027<0459:CEBOSV>2.3.CO;2

De Silva S., and Francis P.W. 'Volcanoes of the Central Andes'. (1991). *21*, Springer-Verlag edition, sec. 6.

DePaolo D.J., 'Trace Element and Isotopic Effects of Combined Wallrock Assimilation and Fractional Crystallization' (1981). *Earth and Planetary Science Letters* 53, 2, 189–202. https://doi.org/10.1016/0012-821X(81)90153-9.

Déruelle B., Figueroa A.O., Medina T.E., Viramonte G.J., and Maragaño C.M. 'Petrology of Pumices of April 1993 Eruption of Lascar (Atacama, Chile)' (1996). *Terra Nova* 8, 2, 191–99. https://doi.org/10.1111/j.1365-3121.1996.tb00744.x.

Díaz D., Brasse H., and Ticona F. 'Conductivity Distribution beneath Lascar Volcano (Northern Chile) and the Puna, Inferred from Magnetotelluric Data' (2012). *J. Volcanol. Geotherm. Res.*217–218, 21–29. https://doi.org/10.1016/j.jvolgeores.2011.12.007.

Dorbath C., and Paul A. 'Tomography of the Andean Crust and Mantle at 20°S: First Results of the Lithoscope Experiment' (1996). *Physics of the Earth and Planetary Interiors* 97, 1, 133–44. https://doi.org/10.1016/0031-9201(96)03140-8.

Elliott T. 'Tracers of the Slab' (2003). *Washington DC American Geophysical Union Geophysical Monograph Series* 138, 23–45. https://doi.org/10.1029/138GM03.

Ewart A., Bryan W.B., Gill J.B. 'Mineralogy and geochemistry of the younger volcanic islands of Tonga, S.W. Pacific' (1973). *J. Petrology* 14, 3, 429-465. https://doi.org/10.1093/petrology/14.3.429

Ewart A., Griffin W.L. 'Application of proton-microprobe data to trace-element partitioning in volcanic rocks' (1994). *Chemical Geology* 117, 1-4, 251-284. 10.1016/0009-2541(94)90131-7.

Francalanci L., Manetti P., Peccerillo A. 'Volcanological and magmatological evolution of Stromboli volcano (Aeolien Islands) : the roles of fractional crystallization, magma mixing, crustal contamination and source heterogeneity' (1989). *Bull. Volc.* 51, 355-378. https://doi.org/10.1007/BF01056897.

Freymuth H., Brandmeier M., and Wörner G.. 'The Origin and Crust/Mantle Mass Balance of Central Andean Ignimbrite Magmatism Constrained by Oxygen and Strontium Isotopes and Erupted Volumes' (2015). *Contrib. Mineral. Petrol*. 169, 6, 58. https://doi.org/10.1007/s00410-015-1152-5.

Gaete A., Cesca S., Franco L., San Martin J., Cartes C., Walter T.R. 'Seismic activity during the 2013-2015 intereruptive phase at Lascar volcano, Chile' (2019). *Geophysical J. International* 219, 1, 449-463. https://doi.org/10.1093/gji/ggz297

Gardeweg, M. C., Sparks R. S. J., and Matthews S. J. 'Evolution of Lascar Volcano, Northern Chile' (1998). *J. Geol. Society* 155, 1, 89–104. https://doi.org/10.1144/gsjgs.155.1.0089.

Godoy B., Wörner B., Kojima S., Aguilera F., Simon K., and Hartmann G.. 'Low-Pressure Evolution of Arc Magmas in Thickened Crust: The San Pedro–Linzor Volcanic Chain, Central Andes, Northern Chile' (2014). J. South American Earth Sciences 52 24–42. https://doi.org/10.1016/j.jsames.2014.02.004.

Godoy B., Wörner G., Le Roux P., De Silva S., Parada M.A., Kojima S., González-Maurel O., Morata D., Polanco E., and Martínez P. 'Sr- and Nd- Isotope Variations along the Pleistocene San Pedro – Linzor Volcanic Chain, N. Chile: Tracking the Influence of the Upper Crustal Altiplano-Puna Magma Body' (2017). *J. Volcanol. Geotherm. Res.*341, 172–86. https://doi.org/10.1016/j.jvolgeores.2017.05.030.

Goss A. R., Kay S.M., and Mpodozis C. 'Andean Adakite-like High-Mg Andesites on the Northern Margin of the Chilean–Pampean Flat-Slab (27–28·5°S) Associated with Frontal Arc Migration and Fore-Arc Subduction Erosion' (2013). *J. Petrology* 54, 11, 2193–2234. https://doi.org/10.1093/petrology/egt044.

Harmon, R. S., Barreiro B. A., Moorbath S., Hoefs J., Francis P. W., Thorpe R. S., Déruelle B., McHugh J., and Viglino J. A.. 'Regional O-, Sr-, and Pb-Isotope Relationships in Late Cenozoic Calc-Alkaline Lavas of the Andean Cordillera' (1984). *J. Geol. Society* 141, 5, 803–22. https://doi.org/10.1144/gsjgs.141.5.0803.

Hartley, A. J. 'Neogene Climate Change and Uplift in the Atacama Desert, Chile: Comment' (2007). *Geology* 35, 1, 120. https://doi.org/10.1130/G23709C.1.

Haschke, M., Siebel W., Günther A., and Scheuber E. 'Repeated Crustal Thickening and Recycling during the Andean Orogeny in North Chile (21°-26°S): Recycling of newly

underplated mafic crust' (2002):. *J. Geophys. Research: Solid Earth* 107, B1, ECV 6-1-ECV 6-18. https://doi.org/10.1029/2001JB000328.

Hickey-Vargas R., Holbik S., Tormey D., Frey F.A., and Moreno H.R. 'Basaltic Rocks from the Andean Southern Volcanic Zone: Insights from the Comparison of along-Strike and Small-Scale Geochemical Variations and Their Sources' (2016). *Lithos* 258–259, 115–32. https://doi.org/10.1016/j.lithos.2016.04.014.

Hidalgo S., Battaglia J., Arellano S., Steele A., Bernard B., Bourquin J., Galle B., Arrais B., and Vásconez F.. 'SO2 Degassing at Tungurahua Volcano (Ecuador) between 2007 and 2013: Transition from Continuous to Episodic Activity' (2015). *J. Volcanol. Geotherm. Res.*298, 1–14. https://doi.org/10.1016/j.jvolgeores.2015.03.022.

Hildreth W., and Moorbath S. 'Crustal Contributions to Arc Magmatism in the Andes of Central Chile'. (1988) Contrib. Mineral. Petrol. 98, 4, 455–89. https://doi.org/10.1007/BF00372365.

Hilton D.R., Hammerschmidt K., Teufel S., and Friedrichsen H. 'Helium Isotope Characteristics of Andean Geothermal Fluids and Lavas' (1993). *Earth and Planetary Science Letters* 120, 3–4, 265–82. https://doi.org/10.1016/0012-821X(93)90244.

Hochstaedter A.G., Gill J.B., Taylor B., Ishizuka O., Yuasa M., and Morita S. 'Accros-arc geochemical trends in the Izu-Bonin arc: Constraints on source composition and mantle melting' (2000). *J. Geophys. Research*. 105, B1, 495-512. https://doi.org/ 10.1029/1999JB900125.

Hofmann A. W. 'Sampling Mantle Heterogeneity through Oceanic Basalts: Isotopes and Trace Elements' (2003). *Treatise on Geochemistry* 2, 568. https://doi.org/10.1016/B0-08-043751-6/02123-X.

Huene, R. von, Weinrebe W., and Heeren F. 'Subduction Erosion along the North Chile Margin' (1999). *J. Geodynamics* 27, 3, 345–58. https://doi.org/10.1016/S0264-3707(98)00002-7.

Jacques, G., Hoernle K., Gill J., Wehrmann H., Bindeman I., and Lara L.E. 'Geochemical Variations in the Central Southern Volcanic Zone, Chile (38–43°S): The Role of Fluids in Generating Arc Magmas' (2014). *Chemical Geology* 371, 27–45. https://doi.org/10.1016/j.chemgeo.2014.01.015.

James, D E. 'The Combined Use of Oxygen and Radiogenic Isotopes as Indicators of Crustal Contamination' (1981). *Annual Review of Earth and Planetary Sciences* 9, 1, 311–44. https://doi.org/10.1146/annurev.ea.09.050181.001523.

Kay S.M., Mpodozis C., Ramos V.A., Munizaga F. 'Magma source variations for mid-late

Tertiary magmatic rocks associated with a shallowing subduction zone and a thickening crust in the central Andes (28 to 33°S)' (1991), Geological Society of America Special Papers 265, 113-138. 10.1130/SPE265-p113.

Kay S.M., 'Tertiary to recent transcient shallow subduction zones in the central and southern' (2002), *Actas del XV congreso geologico Argentino, El Calafate*.

Kay S.M., 'Episodic arc migration, crustal thickening, subduction erosion, and magmatism in the south-central Andes' (2005), *Geological Society of American Bull* 17, 1-2, 67-88. https://doi.org/10.1130/B25431.1

Kay S.M., Mpodozis C., Gardeweg M. 'Magma sources and tectonic setting of Central Andean andesites (25.5-28°S) related to crustal thickening, forearc subduction erosion and delamination' (2014), *Geological Society, London* 385, 1, 303-334. ttps://doi.org/10.1144/SP385.11

Keay S., Collins W. J., and McCulloch M. T. 'A Three-Component Sr-Nd Isotopic Mixing Model for Granitoid Genesis, Lachlan Fold Belt, Eastern Australia' (1997). *Geology* 25, 4, 307–10. https://doi.org/10.1130/0091-7613(1997)025<0307:ATCSNI>2.3.CO;2.

Langmuir C. H., Vocke R.D., Hanson G.N., and Hart S.R. 'A General Mixing Equation with Applications to Icelandic Basalts' (1978). *Earth and Planetary Science Letters* 37, 3, 380–92. https://doi.org/10.1016/0012-821X(78)90053-5.

Lucassen, F., G. Franz, M. F. Thirlwall, and K. Mezger. 'Crustal Recycling of Metamorphic Basement: Late Palaeozoic Granitoids of Northern Chile (∼22°S). Implications for the Composition of the Andean Crust' (1999). *J. Petrology* 40, 10, 1527–51. https://doi.org/10.1093/petroj/40.10.1527.

Lucassen F., Harmon R., Franz G., Romer R.L., Becchio R., and Siebel W. 'Lead Evolution of the Pre-Mesozoic Crust in the Central Andes (18–27°): Progressive Homogenisation of Pb' (2002). *Chemical Geology* 186, 3, 183–97. https://doi.org/10.1016/S0009-2541(01)00407-7.

Mamani M., Tassara A., and Wörner G. 'Composition and Structural Control of Crustal Domains in the Central Andes: Crustal domains in the Central Andes' (2008). *Geochem. Geophy. Geosys.* 9, 3. https://doi.org/10.1029/2007GC001925.

Mamani M., Wörner G., and Sempere T. 'Geochemical Variations in Igneous Rocks of the Central Andean Orocline (13°S to 18°S): Tracing Crustal Thickening and Magma Generation through Time and Space' (2010). *GSA Bulletin* 122, 1–2, 162–82. https://doi.org/10.1130/B26538.1.

Marquillas A.R., Del Papa C., Sabino I.F. 'Sedimentary aspects and paleoenvironmental

evolution of a rift basin: Salta Group (Cretaceous-Paleogene), northwestern Argentina' (2005). *Int. J. Earth Sci* 94, 94-113. https://doi.org/10.1007/s00531-004-0443-2.

Marquillas A.R., Sabino I.F., Sial A.N., Del Papa C., Ferreira V., Matthews S. 'Carbon and oxygen isotopes of Maastrichtian-Danian shallow marine carbonates : Yacoraite formation, northwestern Argentina' (2007). *J. South American Earth Sci.* 23, 304-320 https://doi.org/10.1016/j.jsames.2007.02.009

Mather T. A., Tsanev V. I., Pyle D. M., McGonigle A. J. S, Oppenheimer C., and Allen A. G. 'Characterization and Evolution of Tropospheric Plumes from Lascar and Villarrica Volcanoes, Chile' (2004). *J. Geophy. Research: Atmospheres* 109, D21. https://doi.org/10.1029/2004JD004934.

Matthews S.J., Jones A.P., Gardeweg M.C. 'Lascar volcano, Northern Chile; Evidence for Steady-State Disequilibrium' (1994*). J. Petrology* 35, 2, 401-432. https://doi.org/10.1093/petrology/35.2.401

Matthews S. J., Marquillas R. A., Kemp., A. J, Grange F. K., and Gardeweg M. C. 'Active Skarn Formation beneath Lascar Volcano, Northern Chile: A Petrographic and Geochemical Study of Xenoliths in Eruption Products' (1996). *J. Metamorphic Geology* 14, 4, 509–30. https://doi.org/10.1046/j.1525-1314.1996.00359.x.

Matthews S. J., Stephen J., Gardeweg M.C., and Sparks R.S.J. 'The 1984 to 1996 Cyclic Activity of Lascar Volcano, Northern Chile: Cycles of Dome Growth, Dome Subsidence, Degassing and Explosive Eruptions' (1997). *Bull. Volcanology* 59, 1, 72–82. https://doi.org/10.1007/s004450050176.

Matthews S. J., Sparks R.S.J., and Gardeweg M. C. 'The Piedras Grandes–Soncor Eruptions, Lascar Volcano, Chile; Evolution of a Zoned Magma Chamber in the Central Andean Upper Crust' (1999). *J. Petrology* 40, 12, 1891–1919. https://doi.org/10.1093/petroj/40.12.1891.

McCulloch M. T., and Gamble J. A. 'Geochemical and Geodynamical Constraints on Subduction Zone Magmatism' (1991). *Earth and Planetary Science Letters* 102, 3, 358–74. https://doi.org/10.1016/0012-821X(91)90029-H.

McDonough, W. F., and Sun S. 'The Composition of the Earth' (1995). *Chemical Geology*, Chemical Evolution of the Mantle, 120, 3, 223–53. https://doi.org/10.1016/0009-2541(94)00140-4.

Menard G., Moune S., Vlastélic I., Aguilera F., Valade S., Bontemps M., and González R.. 'Gas and Aerosol Emissions from Lascar Volcano (Northern Chile): Insights into the Origin of Gases and Their Links with the Volcanic Activity' (2014). J. Volcanol. Geotherm.

Res. 287, 51–67. https://doi.org/10.1016/j.jvolgeores.2014.09.004.

Menard G. (2014) 'Comportement des éléments traces au cours des processus de dégazage. Etude des volcans Piton de la Fournaise (Réunion) et Lascar (Chile)'. https://www.theses.fr/2014CLF22460.

Murphy M.D., Sparks R.S.J, Barclay J., Caroll M.R., Lejeune A.-M., Brewer T.S., Macdonald R., Black S., Young S. 'The role of magma mixing in triggering the current eruption at the Soufriere Hills Volcano, Montserrat, West Indies' (1998). *Geophys. Research Letters* 25, 18, 3433-3436. https://doi.org/ 10.1029/98GL00713.

Nauret F., Samaniego P., Ancellin M. -A., Tournigand P. -Y., Le Pennec J. -L., Vlastelic I., Gannoun A., Hidalgo S., and Schiano P. 'The Genetic Relationship between Andesites and Dacites at Tungurahua Volcano, Ecuador' (2017). *J. Volcanol. Geotherm. Res.* 349, 283–97. https://doi.org/10.1016/j.jvolgeores.2017.11.012.

Pavez A., Remy D., Bonvalot S., Diament M., Gabalda G., Froger J.L., Julien P., Legrand D., Moisset D. 'Insight into ground deformation at Lascar volcano (Chile) from SAR interferometry, photogrammetry and GPS data : Implications on volcano dynamics and future space monitoring' (2006). *Remote Sensing of Environment* 100, 3, 307-320. https://doi.org/10.1016/j.rse.2005.10.013

Peccerillo A., Taylor S.R., 'Geochemistry of Eocene calc-alkaline volcanic rocks from the Kastamonu area, northern Turkey' (1976). *Contrib. Mineral. Petrol.* 58, 1, 63-81. https://doi.org/10.1007/BF00384745

Pin C., Gannoun A., and Dupont A. 'Rapid, Simultaneous Separation of Sr, Pb, and Nd by Extraction Chromatography Prior to Isotope Ratios Determination by TIMS and MC-ICP-MS' (2014). *J. Analytical Atomic Spectrometry* 29, 10, 1858–70. https://doi.org/10.1039/C4JA00169A.

Plank T., and Langmuir C.H. 'The Chemical Composition of Subducting Sediment and its Consequences for the Crust and Mantle' (1998). Chemical Geology 145, 3, 325–94. https://doi.org/10.1016/S0009-2541(97)00150-2.

Philpotts, J.A., Schnetzler, C.C. 'Phenocryst-matrix partition coefficients for K, Rb, Sr and Ba, with applications to anorthosite and basalt genesis' (1970). *GCA* 34, 3, 307-322. 10.1016/0016-7037(70)90108-0.

Rawson H. 'Compositional Variability in Mafic Arc Magmas over Short Spatial and Temporal Scales: Evidence for the Signature of Mantle Reactive Melt Channels' (2016). Earth and Planetary Science Letters 456, 66-77, https://doi.org/10.1016/j.epsl.2016.09.056.

Richter N., Salzer J.T., Zeew-van Dalfsen E., Perissin D., Walter T.R. 'Constraints on the

geomorphological evolution of the nested summit craters of Lascar volcano from high spatio-temporal resolution TerraSAR-X interferometry' (2018). *Bull. Volc.* 80, 3, 21. https://doi.org/10.1007/s00445-018-1195-3

Rech J.A., Currie B.S., Michalski G., and Cowan A.M. 'Neogene Climate Change and Uplift in the Atacama Desert, Chile' (2006). *Geology* 34, 9, 761–64. https://doi.org/10.1130/G22444.1.

Rehkämper M., and Hofmann A. W. 'Recycled Ocean Crust and Sediment in Indian Ocean MORB' (1997). *Earth and Planetary Science Letters* 147, 1, 93–106. https://doi.org/10.1016/S0012-821X(97)00009-5.

Risacher F., and Alonso H. 'Geochemistry of Ash Leachates from the 1993 Lascar Eruption, Northern Chile. Implication for Recycling of Ancient Evaporites' (2001). *J. Volcanol. Geotherm. Res.*109, 4, 319–37. https://doi.org/10.1016/S0377-0273(01)00198-6.

Rogers G., Hawkesworth CJ. 'A geochemical traverse across the North Chilean Andes : Evidence for crust generation from the mantle wedge' (1989). Earth and Planetary Science Letters 91, 3-4, 271-285. https://doi.org/10.1016/0012-821X(89)90003-4

Rosner M., Erzinger J., Franz G., and Trumbull R.B. 'Slab-Derived Boron Isotope Signatures in Arc Volcanic Rocks from the Central Andes and Evidence for Boron Isotope Fractionation during Progressive Slab Dehydration: Slab-derived boron isotope signatures' (2003). *Geochem. Geophy. Geosys.* 4, 8 https://doi.org/10.1029/2002GC000438.

Schiano P., Monzier M., Eissen J.-P., Martin H., and Koga K. T.. 'Simple Mixing as the Major Control of the Evolution of Volcanic Suites in the Ecuadorian Andes'(2010). *Contrib. Mineral. Petrol*. 160, 2, 297–312. https://doi.org/10.1007/s00410-009-0478-2.

Siebel W., Schnurr B. W., Hahne K., Kraemer B., Trumbull R.B., Van den Bogaard P., and Emmermann R. 'Geochemistry and Isotope Systematics of Small- to Medium-Volume Neogene–Quaternary Ignimbrites in the Southern Central Andes: Evidence for Derivation from Andesitic Magma Sources' (2001). *Chemical Geology* 171, 3, 213–37. https://doi.org/10.1016/S0009-2541(00)00249-7.

Snyder D. 'Thermal effects of the intrusion of basaltic magma into a more silicic magma chamber and implications for eruption triggering' (2000). *Earth and Planetary Science Letters* 175, 3-4, 257-273. https://doi.org/10.1016/S0012-821X(99)00301-5.

Sparks S.R.J. 'Magma mixing: a mechanism for triggering acid explosive eruptions' (1977). *Nature* 267, 5609, 315-318. https://doi.org/ 10.1038/267315a0.

Spiegelman M., and Kelemen P.B. 'Extreme Chemical Variability as a Consequence of

Channelized Melt Transport: Channel-induced chemical variation' (2003). *Geochem. Geophy. Geosys.* 4, 7. https://doi.org/10.1029/2002GC000336.

Stern C.R.'Role of subduction erosion in the generation of Andean magmas' (1991). *Geology* 19, 78-81. https://doi.org/10.1130/0091-7613(1991)019<0078:ROSEIT>2.3.CO;2

Stern C.R. 'Active Andean Volcanism: Its Geologic and Tectonic Settings' (2004). *Revista Geológica de Chile* 31, 2, 161–206. https://doi.org/10.4067/S0716-02082004000200001.

Sun S.S., and McDonough W.F. 'Chemical and isotopic systematics of oceanic basalts: implications for mantle composition and processes' (1989). *Geological Society*, 42, 313-345. https://doi.org/10.1144/GSL.SP.1989.042.01.19

Tassi, F., Aguilera F., Vaselli O., Medina E., Tedesco D., Delgado Huertas A., Poreda R., and Kojima S. 'The Magmatic- and Hydrothermal-Dominated Fumarolic System at the Active Crater of Lascar Volcano, Northern Chile' (2009). *Bull. Volcanology* 71, 2, 171–83. https://doi.org/10.1007/s00445-008-0216-z.

Tiepolo M., Oberti R., Zanetti A., Vannucci R., Foley S.F. 'Trace-element partitioning between amphibole and silicate melt'(2007). *Reviews in Mineralogy and Geochemistry* 67, 1, 417-452. https://doi.org/10.2138/rmg.2007.67.11

Todt, W., Cliff R. A., Hanser A., and Hofmann A. W. 'Evaluation of a ^{202}Pb–^{205}Pb Double Spike for High - Precision Lead Isotope Analysis.*' (2013). In *Earth Processes: Reading the Isotopic Code*, 429–37. American Geophysical Union (AGU), https://doi.org/10.1029/GM095p0429.

Turner S.J., and Langmuir C.H. 'The Global Chemical Systematics of Arc Front Stratovolcanoes: Evaluating the Role of Crustal Processes' (2015). *Earth and Planetary Science Letters* 422, 182–93. https://doi.org/10.1016/j.epsl.2015.03.056.

Unruh D., Tatsumoto M.M., Initial Reports of the Deep Sea Drilling Project, 34 (1976), 34. *Initial Reports of the Deep Sea Drilling Project*. U.S. Government Printing Office, https://doi.org/10.2973/dsdp.proc.34.1976.

Vatin-Pérignon N., Oliver R.A., Goemans P., Keller F., Briqueu L., and Guido Salas A. 'Geodynamic Interpretations of Plate Subduction in the Northernmost Part of the Central Volcanic Zone from the Geochemical Evolution and Quantification of the Crustal Contamination of the Nevado Solimana Volcano, Southern Peru' (1992). Tectonophysics, Andean geodynamics, 205, 1, 329–55. https://doi.org/10.1016/0040-1951(92)90434-8.

Weber M.B., Tarney J.I, Kempton P.D., and Kent R.W. 'Crustal Make-up of the Northern

Andes: Evidence Based on Deep Crustal Xenolith Suites, Mercaderes, SW Colombia' (2002). *Tectonophysics*, Andean Geodynamics ISAG 4, 345, 1, 49–82. https://doi.org/10.1016/S0040-1951(01)00206-2.

Wendt J.I., Regelous M., Niu Y., Hékinian R., and Collerson K.D. 'Geochemistry of Lavas from the Garrett Transform Fault: Insights into Mantle Heterogeneity beneath the Eastern Pacific' (1999). *Earth and Planetary Science Letters* 173, 3, 271–84. https://doi.org/10.1016/S0012-821X(99)00236-8.

Wörner, G., Harmon R. S., Davidson J., Moorbath S., Turner D. L., McMillan N., Nyes C., Lopez-Escobar L., and Moreno H. 'The Nevados de Payachata Volcanic Region (18°S/69°W, N. Chile)' (1988). *Bull. Volcanology* 50, 5, 287–303. https://doi.org/10.1007/BF01073587.

Wörner G., Moorbath S., Harmon R.S. 'Andean Cenozoic Volcanic Centers Reflect Basement Isotopic Domains' (1992). *Geology* 20, 12, 1103–6. https://doi.org/10.1130/0091-7613(1992)020<1103:ACVCRB>2.3.CO;2.

Wörner G., Moorbath S., Horn S., Entenmann J., Harmon R.S., Davidson J.P., and Lopez-Escobar L. 'Large- and Fine-Scale Geochemical Variations Along the Andean Arc of Northern Chile (17.5°– 22°S)' (1994). In *Tectonics of the Southern Central Andes: Structure and Evolution of an Active Continental Margin*, 77–92. https://doi.org/10.1007/978-3-642-77353-2_5.

Worner G., Mamani M., Hartmann G., and Simon K. 'Regional Patterns 'in Arc Magma Composition in the Andean Central Volcanic Zone (13°5-28°5)', (2005) *6th International Symposium on Andean Geodynamics*.

Zeeuw-van Dalfsen E., Richter N., Gonzalez G., Walter T.R. 'Geomorphology and structural development of the nested summit crater of Lascar volcano studied with Terrestrial Laser Scanner data and analogue modelling' (2017). *J. Volc. Geotherm. Res*. 329, 1-12. https://doi.org/10.1016/j.jvolgeores.2016.09.018

Zellmer, Georg F., Pistone M., Iizuka Y., Andrews B.J., Gómez-Tuena A., Straub S.M., and Cottrell E. 'Petrogenesis of Antecryst-Bearing Arc Basalts from the Trans-Mexican Volcanic Belt: Insights into along-Arc Variations in Magma-Mush Ponding Depths, H_2O Contents, and Surface Heat Flux' (2016). *American Mineralogist* 101, 11, 2405–22. https://doi.org/10.2138/am-2016-5701.

Figure 1

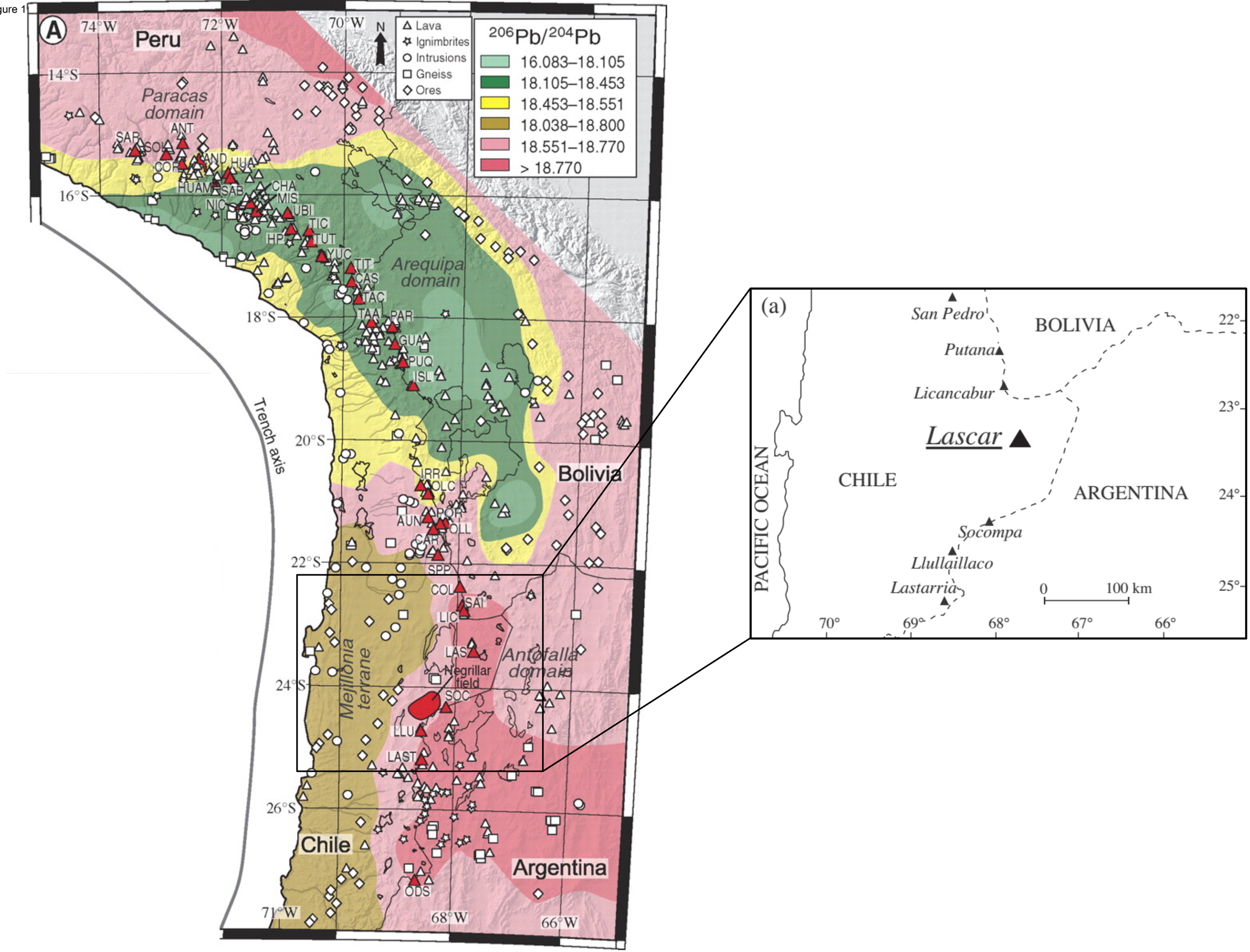
A
74°W
72°W
70°W
N
Peru
14°S
16°S
18°S
20°S
22°S
24°S
26°S
Lava
Ignimbrites
Intrusions
Gneiss
Ores
206Pb/204Pb
16.083–18.105
18.105–18.453
18.453–18.551
18.038–18.800
18.551–18.770
> 18.770
Paracas domain
Arequipa domain
Mejillonia terrane
Antofalla domain
Negrillar field
Trench axis
Bolivia
Chile
Argentina
ANT
SAR
SOL
COR
AND
HUA
HUAM
SAB
CHA
MIS
NIC
UBI
TIC
HP
TUT
YUC
TIT
CAS
TAC
TAA
PAR
GUA
PUQ
ISL
IRR
VOLC
APOR
AUN
OLL
CAR
SPP
COL
SAI
LIC
LAS
SOC
LLU
LAST
ODS
71°W
68°W
66°W
(a)
San Pedro
Putana
Licancabur
Lascar
BOLIVIA
CHILE
ARGENTINA
PACIFIC OCEAN
Socompa
Llullaillaco
Lastarria
0
100 km
22°
23°
24°
25°
70°
69°
68°
67°
66°

Figure 2

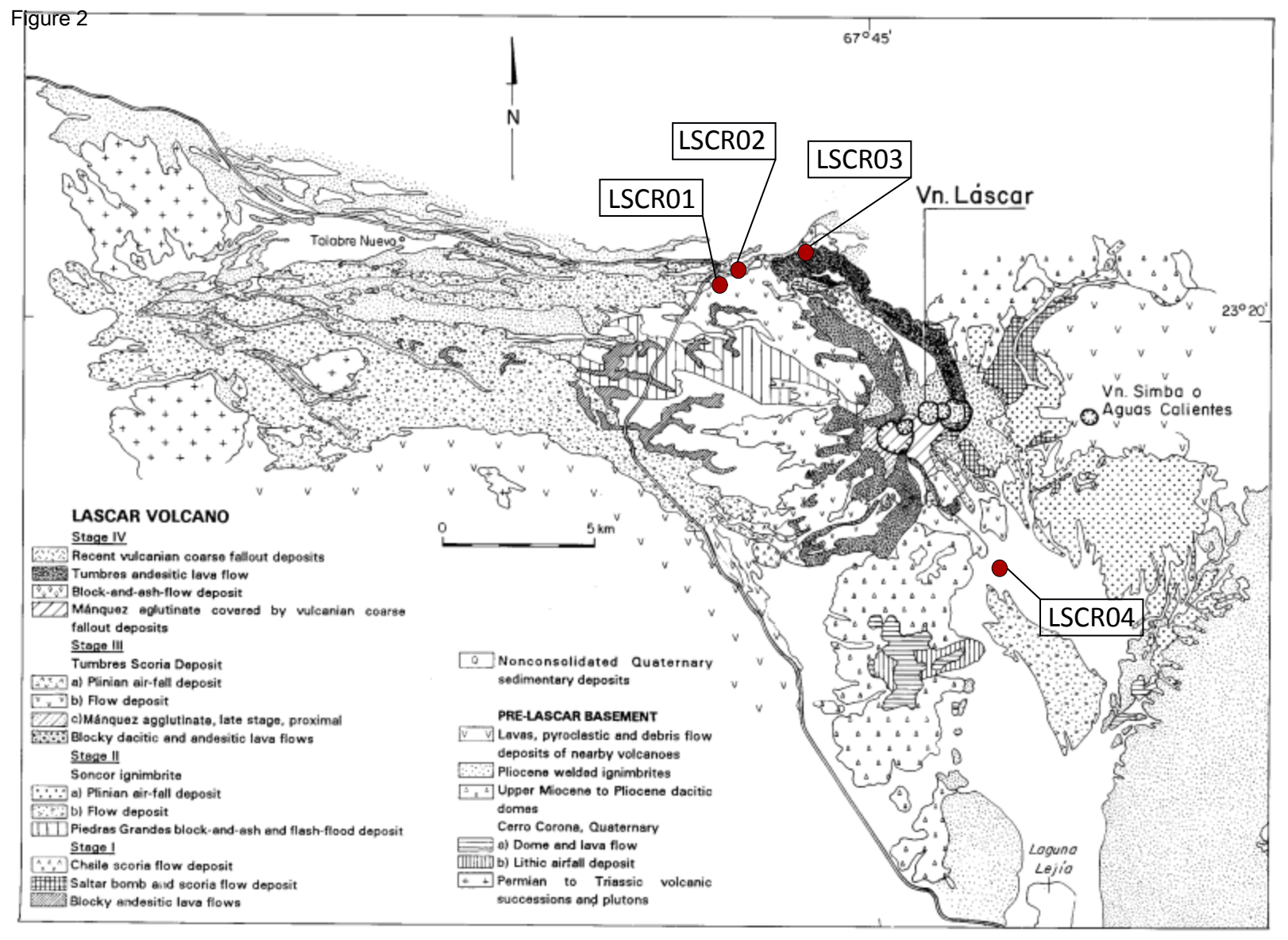
67°45'
N
LSCR01
LSCR02
LSCR03
LSCR04
Vn. Láscar
Tolabre Nuevo
23°20'
Vn. Simbo o
Aguas Calientes
0
5 km
Laguna
Lejía
LASCAR VOLCANO
Stage IV
Recent vulcanian coarse fallout deposits
Tumbres andesitic lava flow
Block-and-ash-flow deposit
Mánquez aglutinate covered by vulcanian coarse fallout deposits
Stage III
Tumbres Scoria Deposit
a) Plinian air-fall deposit
b) Flow deposit
c) Mánquez agglutinate, late stage, proximal
Blocky dacitic and andesitic lava flows
Stage II
Soncor ignimbrite
a) Plinian air-fall deposit
b) Flow deposit
Piedras Grandes block-and-ash and flash-flood deposit
Stage I
Chaile scoria flow deposit
Saltar bomb and scoria flow deposit
Blocky andesitic lava flows
Q Nonconsolidated Quaternary sedimentary deposits
PRE-LASCAR BASEMENT
Lavas, pyroclastic and debris flow deposits of nearby volcanoes
Pliocene welded ignimbrites
Upper Miocene to Pliocene dacitic domes
Cerro Corona, Quaternary
a) Dome and lava flow
b) Lithic airfall deposit
Permian to Triassic volcanic successions and plutons

Figure 4

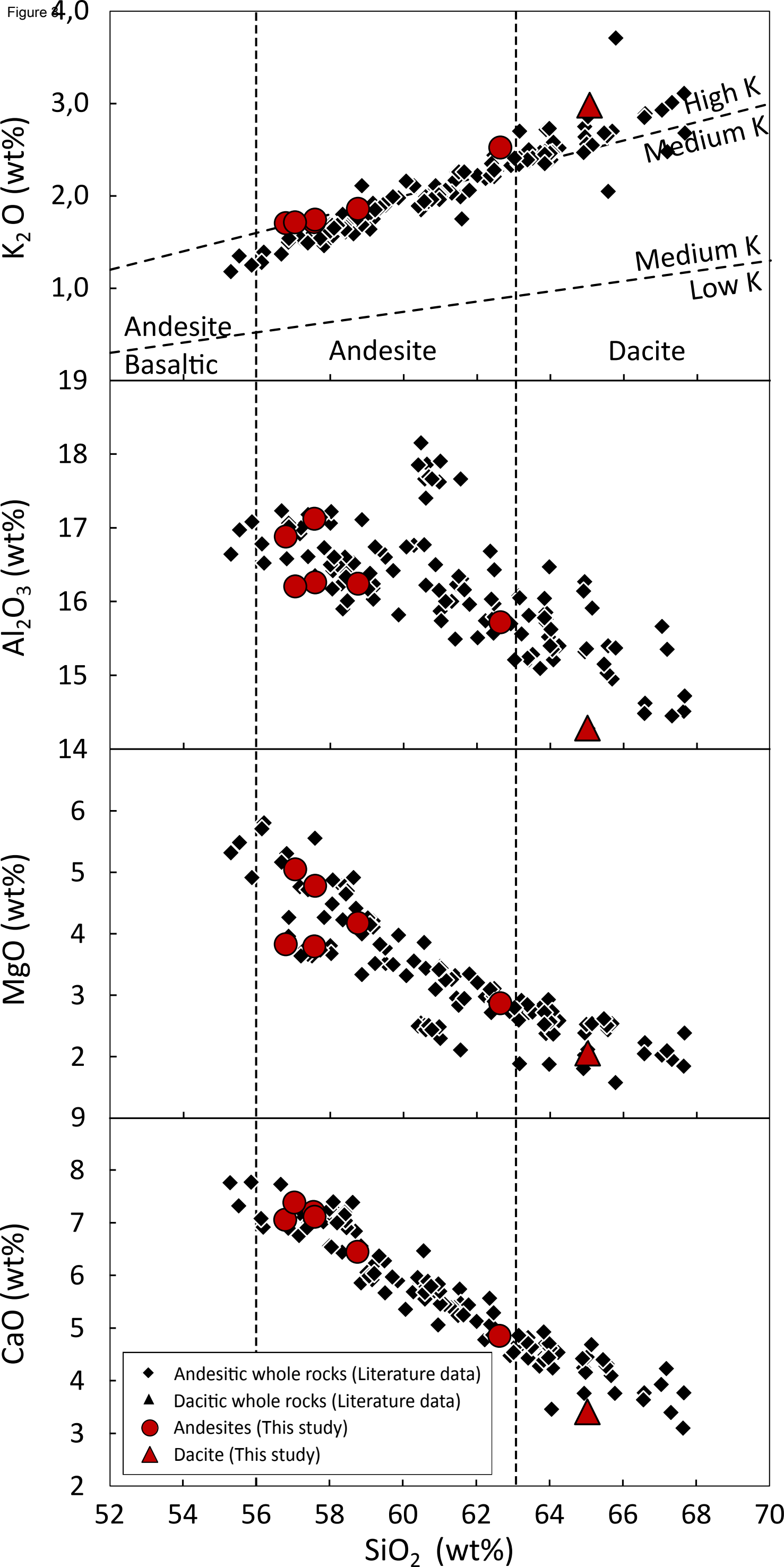
K_2O (wt%)
4,0
3,0
2,0
1,0
19
High K
Medium K
Medium K
Low K
Andesite
Basaltic
Andesite
Dacite
Al_2O_3 (wt%)
18
17
16
15
14
MgO (wt%)
6
5
4
3
2
9
CaO (wt%)
8
7
6
5
4
3
2
Andesitic whole rocks (Literature data)
Dacitic whole rocks (Literature data)
Andesites (This study)
Dacite (This study)
52
54
56
58
60
62
64
66
68
70
SiO_2 (wt%)

Figure 4

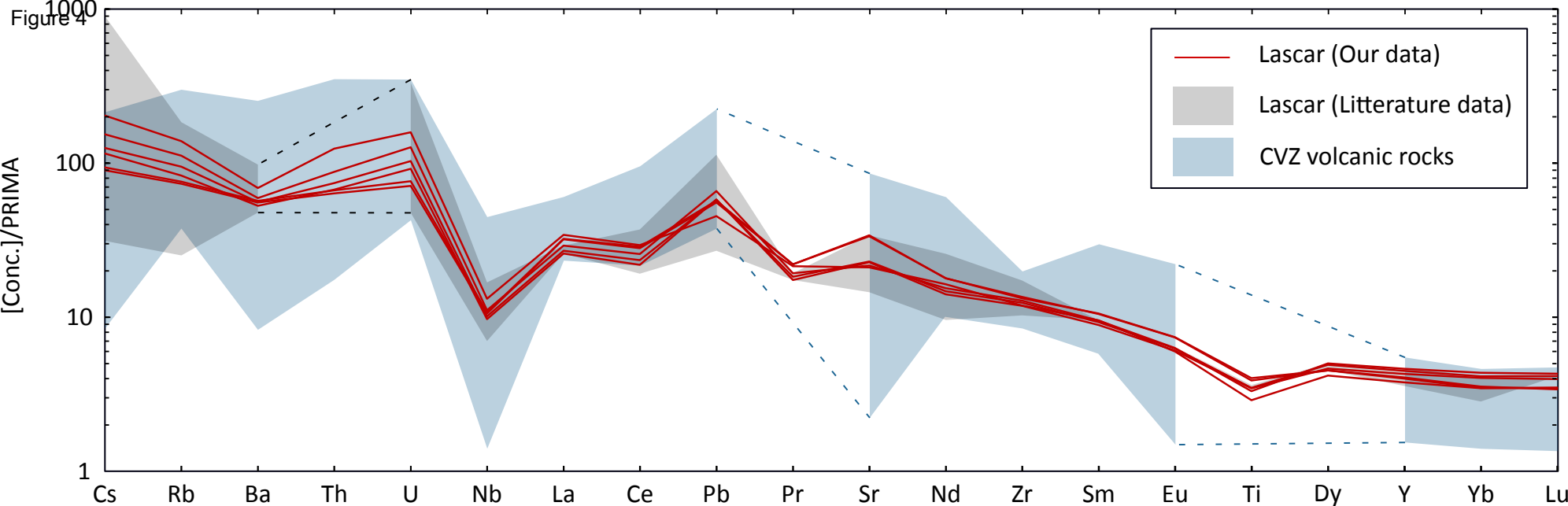
Lascar (Our data)
Lascar (Litterature data)
CVZ volcanic rocks
[Conc.]/PRIMA
1000
100
10
1
Cs
Rb
Ba
Th
U
Nb
La
Ce
Pb
Pr
Sr
Nd
Zr
Sm
Eu
Ti
Dy
Y
Yb
Lu

Figure 5

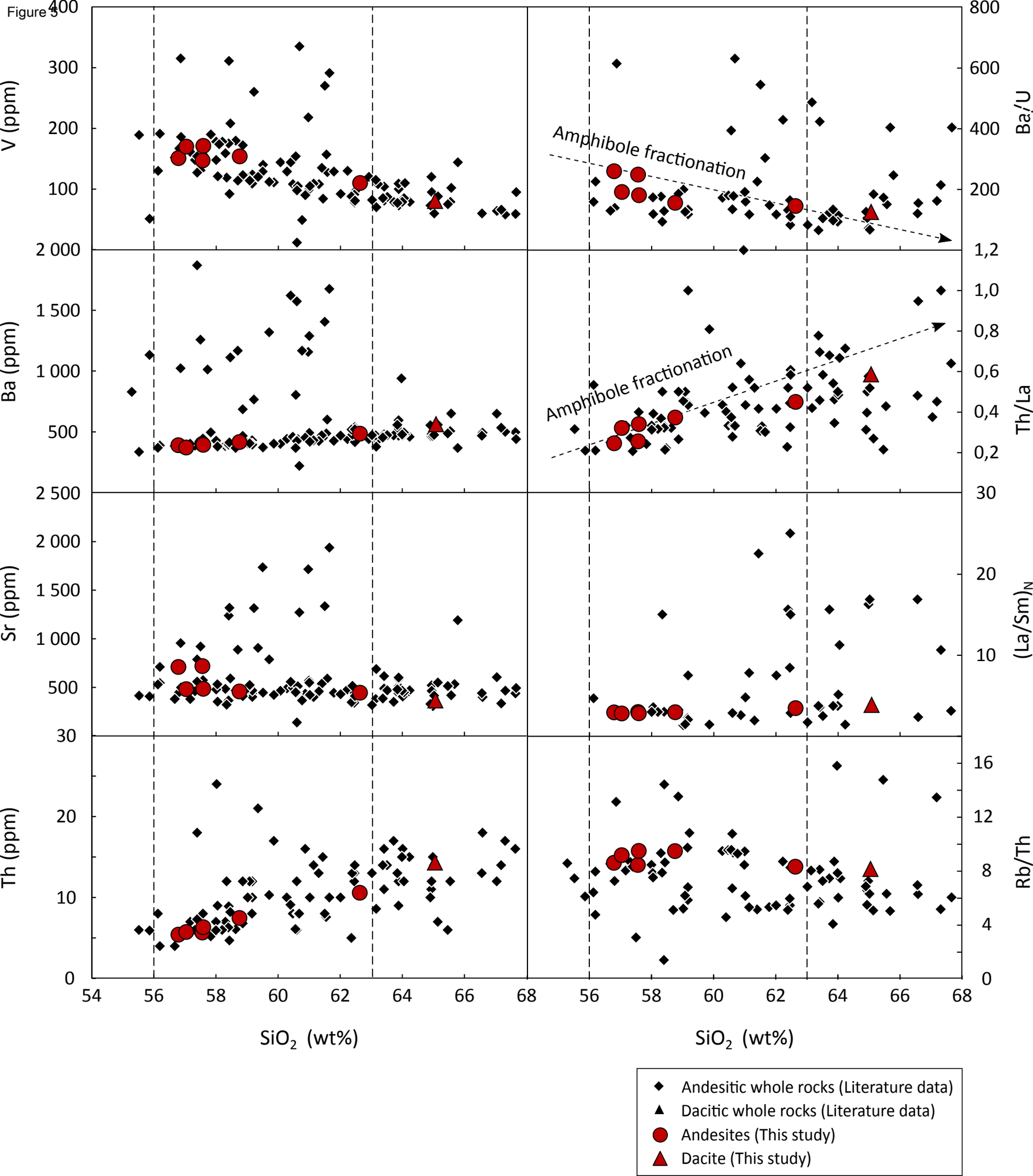
V (ppm)
Ba/U
Amphibole fractionation
Ba (ppm)
Th/La
Amphibole fractionation
Sr (ppm)
(La/Sm)N
Th (ppm)
Rb/Th
SiO2 (wt%)
SiO2 (wt%)
Andesitic whole rocks (Literature data)
Dacitic whole rocks (Literature data)
Andesites (This study)
Dacite (This study)

Figure 6

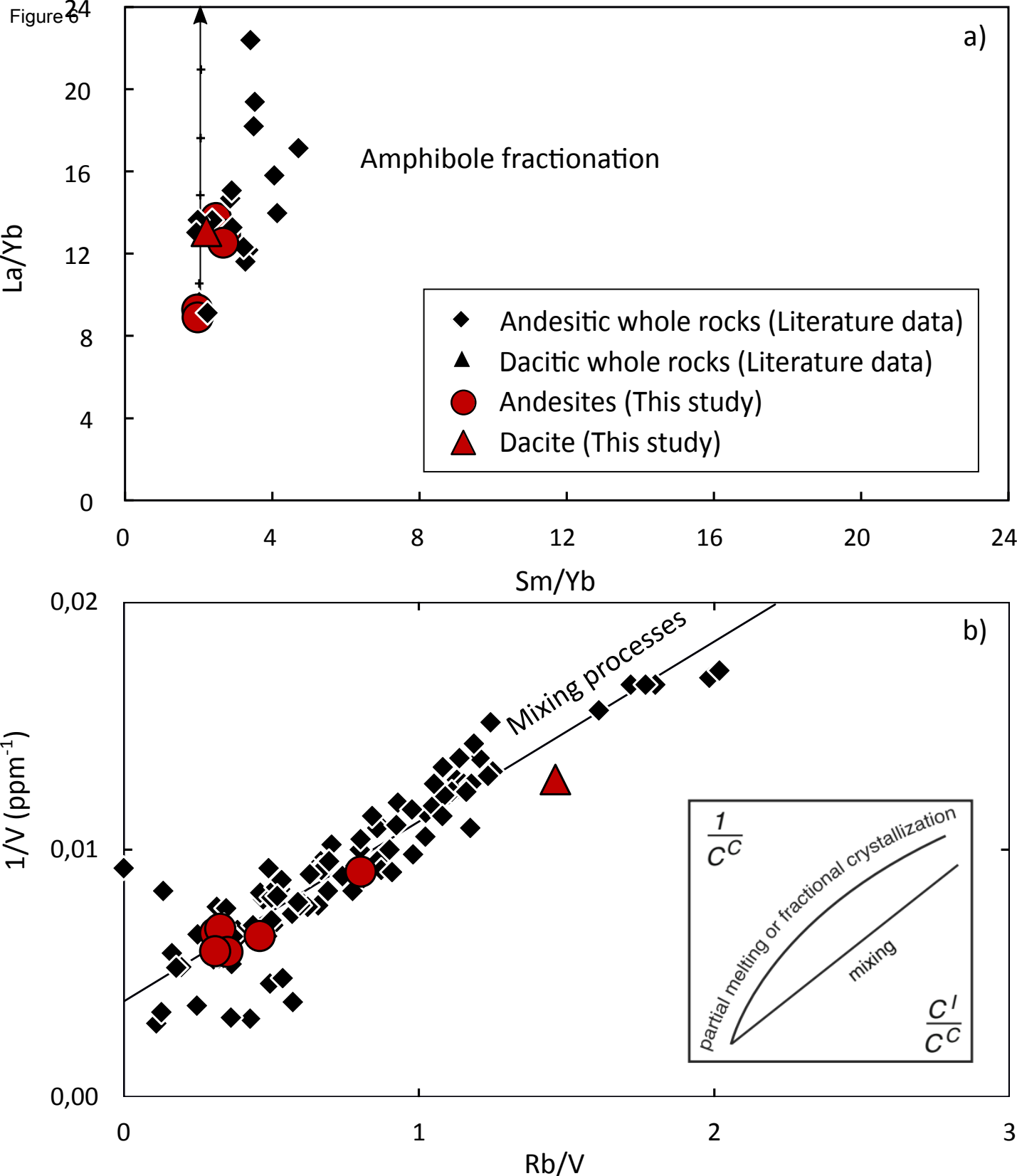
a)
Amphibole fractionation
La/Yb
Sm/Yb
0
4
8
12
16
20
24
Andesitic whole rocks (Literature data)
Dacitic whole rocks (Literature data)
Andesites (This study)
Dacite (This study)
b)
Mixing processes
1/V (ppm-1)
Rb/V
0,00
0,01
0,02
0
1
2
3
1/C^C
partial melting or fractional crystallization
mixing
C^I/C^C

Figure

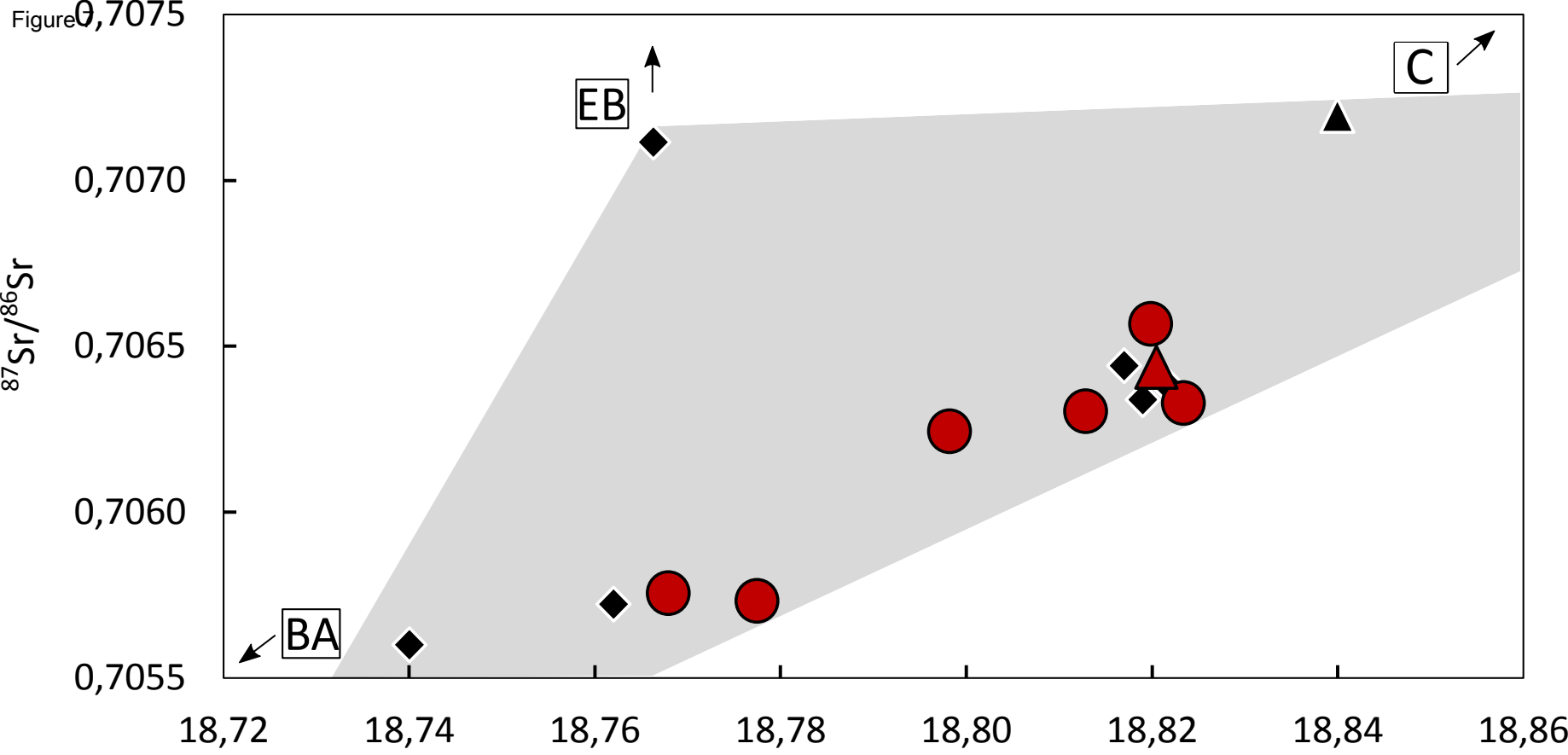
0,7075
0,7070
0,7065
0,7060
0,7055
$^{87}Sr/^{86}Sr$
EB
C
BA
18,72
18,74
18,76
18,78
18,80
18,82
18,84
18,86
$^{206}Pb/^{204}Pb$

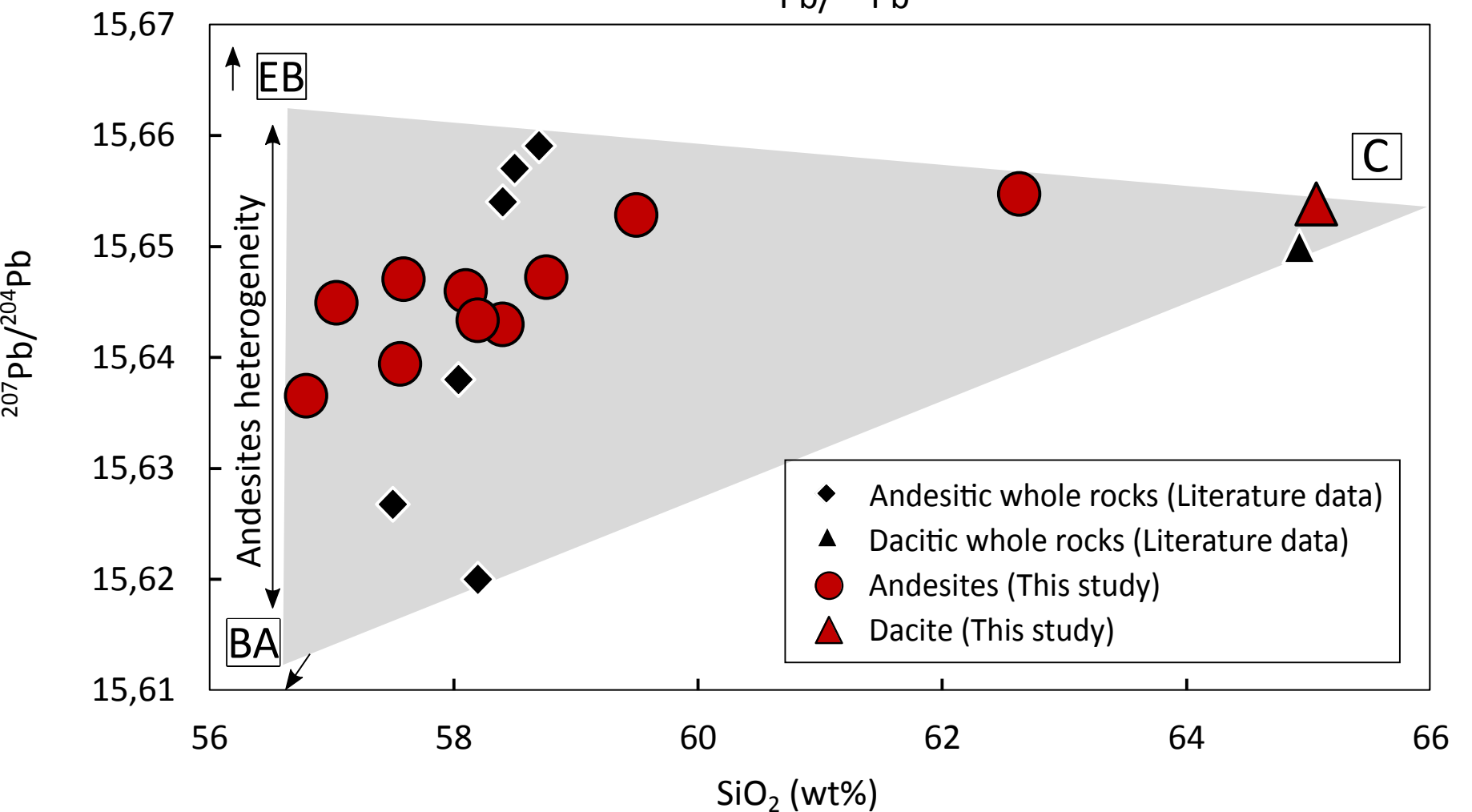
15,67
15,66
15,65
15,64
15,63
15,62
15,61
$^{207}Pb/^{204}Pb$
EB
C
BA
Andesites heterogeneity
Andesitic whole rocks (Literature data)
Dacitic whole rocks (Literature data)
Andesites (This study)
Dacite (This study)
56
58
60
62
64
66
SiO_2 (wt%)

Figure 8

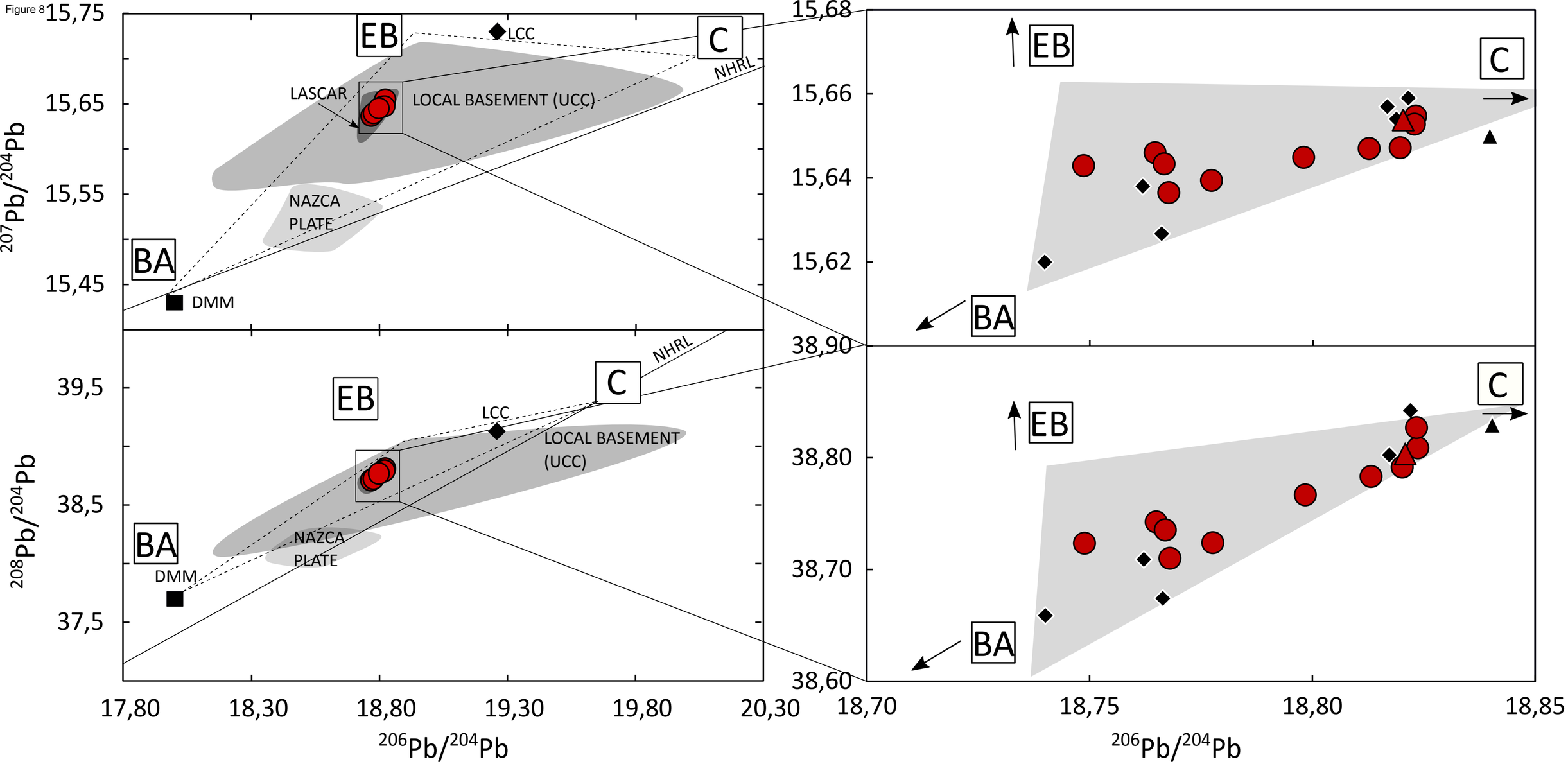
EB
C
BA
LCC
NHRL
LASCAR
LOCAL BASEMENT (UCC)
NAZCA
PLATE
DMM
LOCAL BASEMENT
(UCC)
15,75
15,65
15,55
15,45
39,5
38,5
37,5
17,80
18,30
18,80
19,30
19,80
20,30
15,68
15,66
15,64
15,62
38,90
38,80
38,70
38,60
18,70
18,75
18,80
18,85
207Pb/204Pb
208Pb/204Pb
206Pb/204Pb
Andesitic whole rocks (Literature data)
Dacitic whole rocks (Literature data)
Andesites (This study)
Dacite (This study)

Figure 9

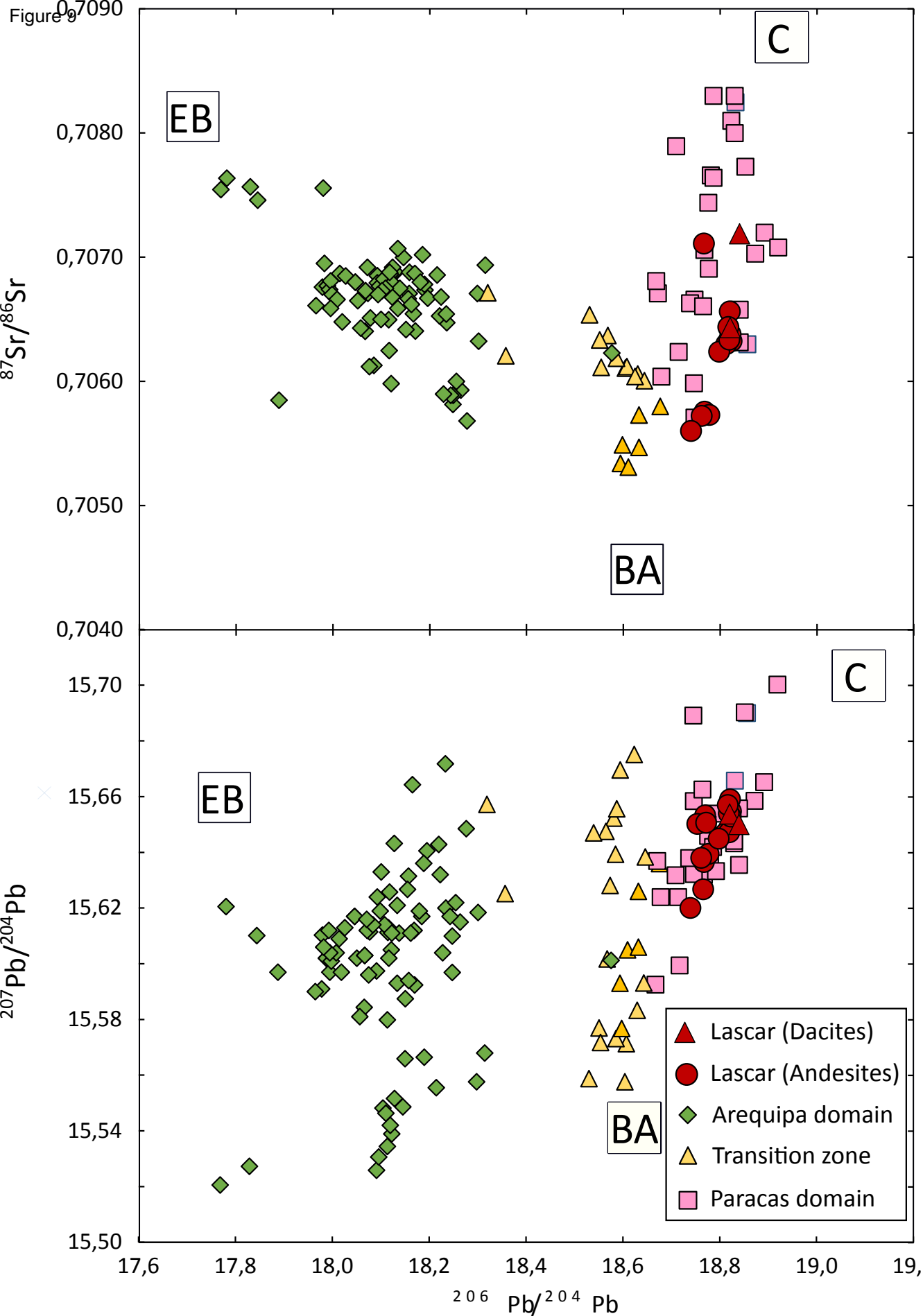
C
EB
BA
0,7090
0,7080
0,7070
0,7060
0,7050
0,7040
$^{87}Sr/^{86}Sr$
C
EB
BA
15,70
15,66
15,62
15,58
15,54
15,50
$^{207}Pb/^{204}Pb$
Lascar (Dacites)
Lascar (Andesites)
Arequipa domain
Transition zone
Paracas domain
17,6
17,8
18,0
18,2
18,4
18,6
18,8
19,0
19,2
$^{206}Pb/^{204}Pb$

Figure 10

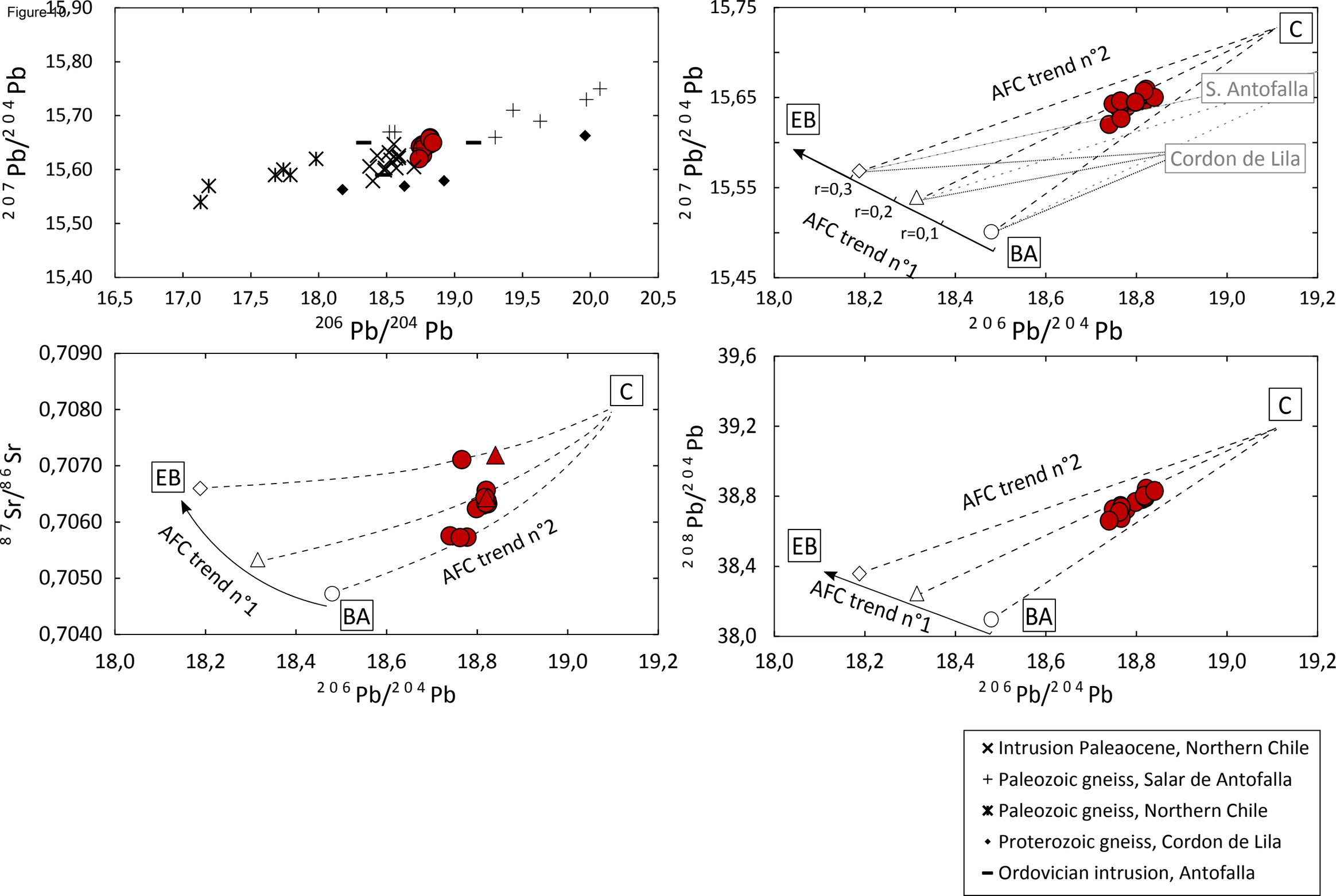
15,90
15,80
15,70
15,60
15,50
15,40
207 Pb/204 Pb
16,5
17,0
17,5
18,0
18,5
19,0
19,5
20,0
20,5
206 Pb/204 Pb
15,75
15,65
15,55
15,45
207 Pb/204 Pb
C
AFC trend n°2
S. Antofalla
EB
Cordon de Lila
r=0,3
r=0,2
r=0,1
AFC trend n°1
BA
18,0
18,2
18,4
18,6
18,8
19,0
19,2
206 Pb/204 Pb
0,7090
0,7080
0,7070
0,7060
0,7050
0,7040
87 Sr/86 Sr
C
EB
AFC trend n°1
AFC trend n°2
BA
18,0
18,2
18,4
18,6
18,8
19,0
19,2
206 Pb/204 Pb
39,6
39,2
38,8
38,4
38,0
208 Pb/204 Pb
C
AFC trend n°2
EB
AFC trend n°1
BA
18,0
18,2
18,4
18,6
18,8
19,0
19,2
206 Pb/204 Pb
Intrusion Paleaocene, Northern Chile
Paleozoic gneiss, Salar de Antofalla
Paleozoic gneiss, Northern Chile
Proterozoic gneiss, Cordon de Lila
Ordovician intrusion, Antofalla

Figure 11

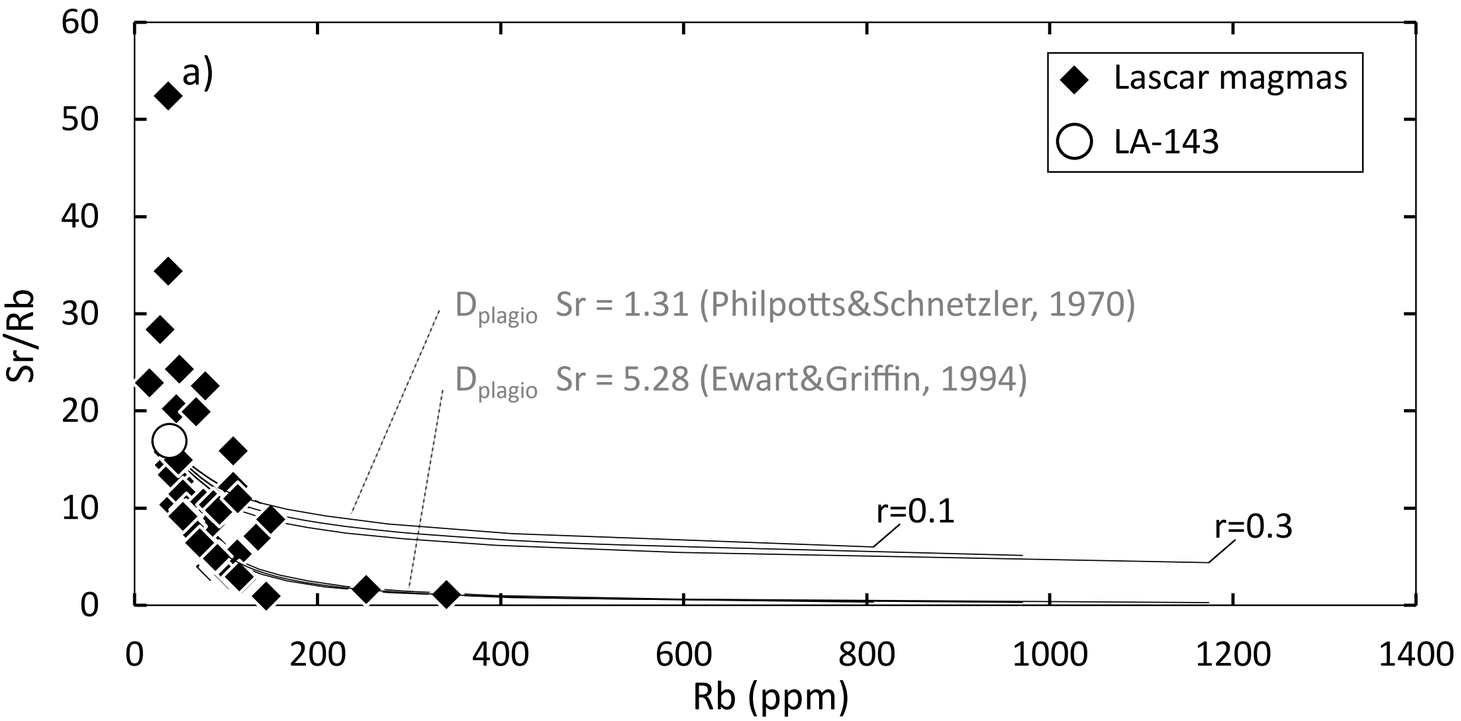
a)
Lascar magmas
LA-143
D_{plagio} Sr = 1.31 (Philpotts&Schnetzler, 1970)
D_{plagio} Sr = 5.28 (Ewart&Griffin, 1994)
r=0.1
r=0.3
Sr/Rb
Rb (ppm)
0
10
20
30
40
50
60
0
200
400
600
800
1000
1200
1400

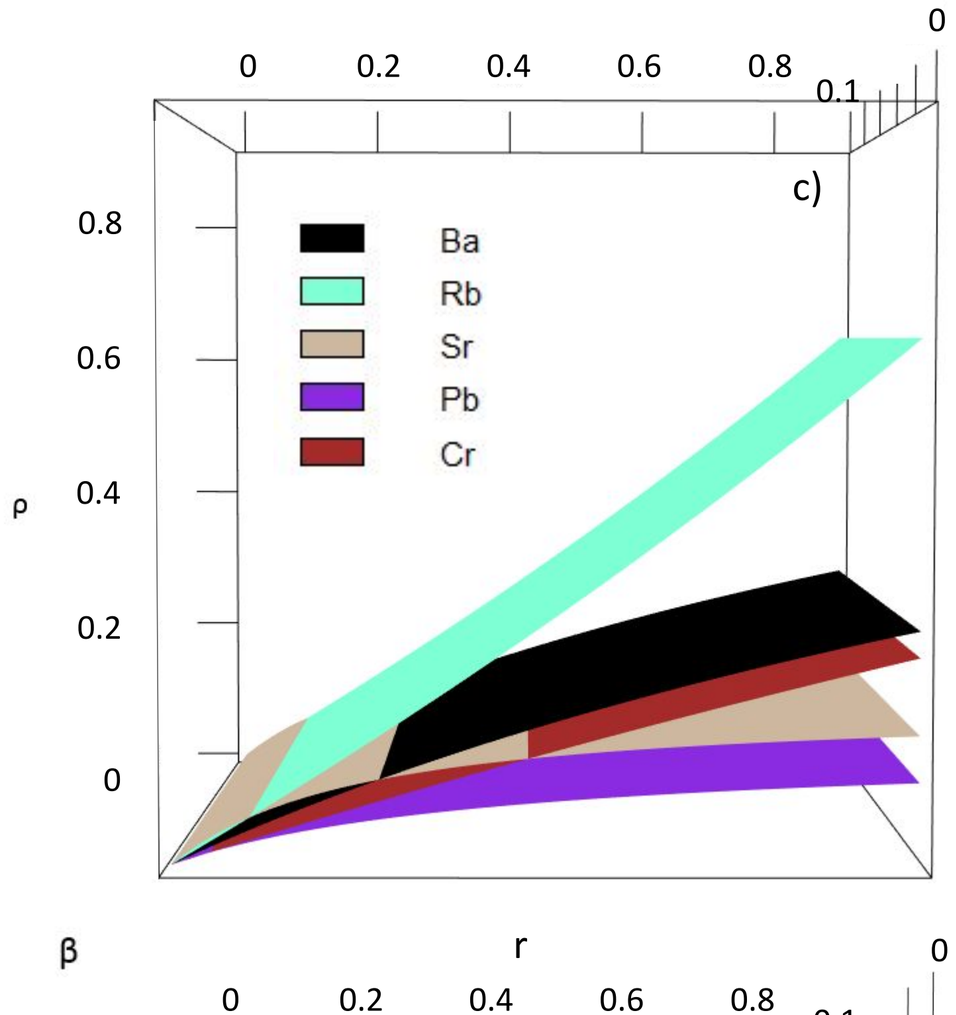
c)
Ba
Rb
Sr
Pb
Cr
ρ
β
r
0
0.2
0.4
0.6
0.8
0.1

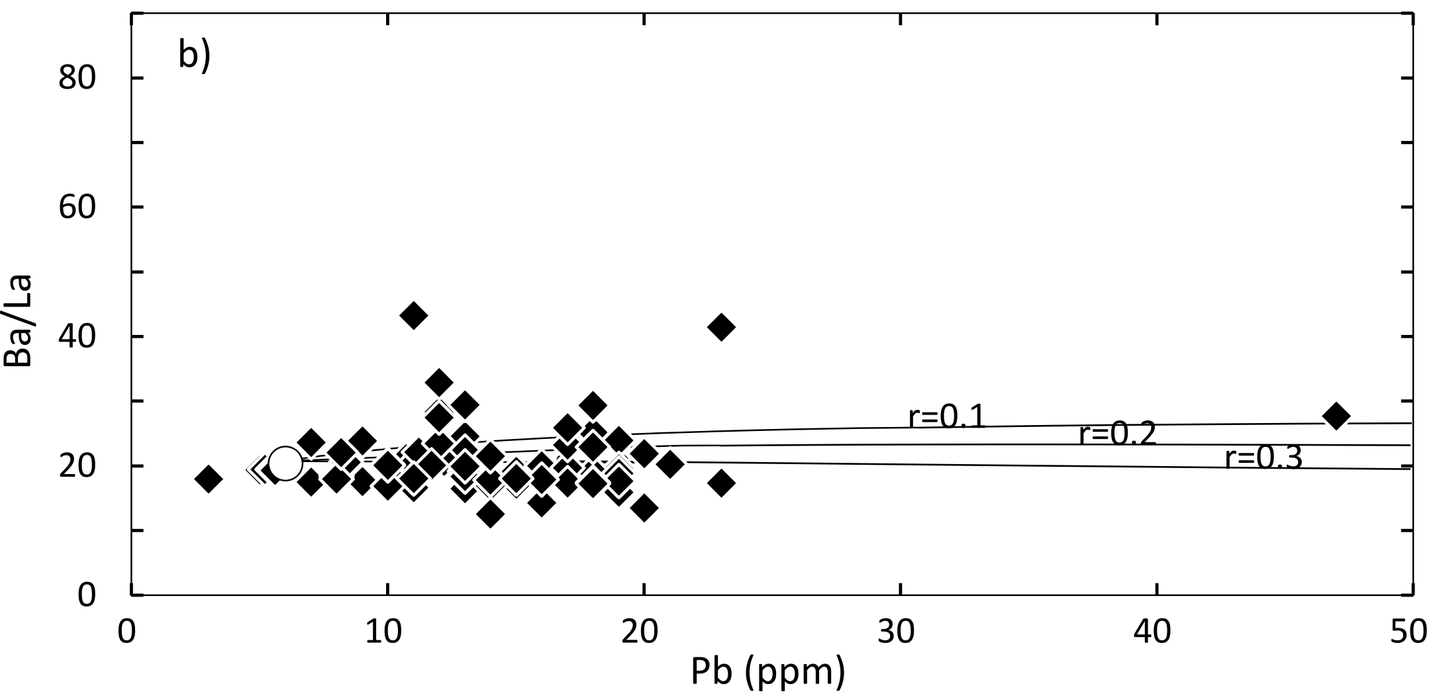
b)
r=0.1
r=0.2
r=0.3
Ba/La
Pb (ppm)
0
10
20
30
40
50
60
80

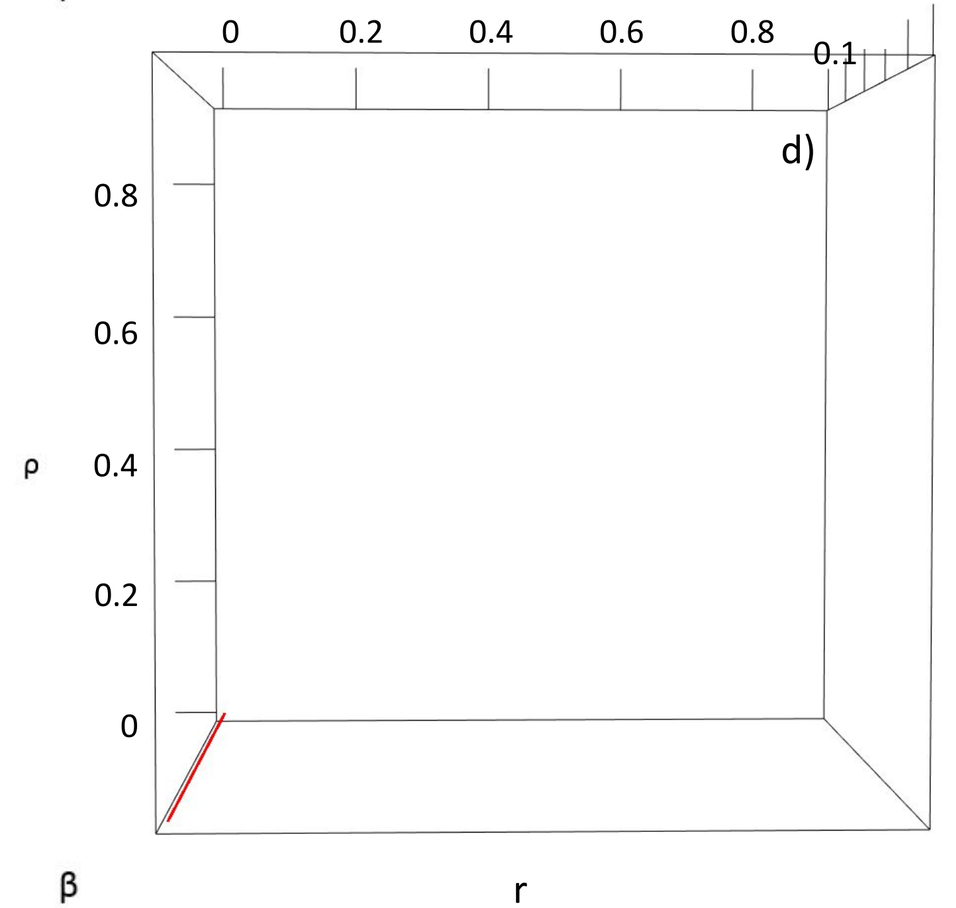
d)
ρ
β
r
0
0.2
0.4
0.6
0.8
0.1